

This is the preprint version of the contribution published as:

Wu, L., Verma, D., Bondgaard, M., Melvej, A., Vogt, C., Subudhi, S., Richnow, H.H.
(2018):

Carbon and hydrogen isotope analysis of parathion for characterizing its natural attenuation
by hydrolysis at a contaminated site

Water Res. **143**, 146 – 154

The publisher's version is available at:

<http://dx.doi.org/10.1016/j.watres.2018.06.039>

1 **Carbon and hydrogen isotope analysis of parathion for characterizing its natural**
2 **attenuation by hydrolysis at a contaminated site**

3 Langping Wu^a, Dipti Verma^b, Morten Bondgaard^c, Anja Melvej^c, Carsten Vogt^a, Sanjukta
4 Subudhi^b, Hans H. Richnow^{a,*}

5 ^a Department of Isotope Biogeochemistry, Helmholtz Centre for Environmental Research-UFZ,
6 Permoserstraße 15, 04318 Leipzig, Germany

7 ^b Environmental and Industrial Biotechnology Division, The Energy and Resources Institute,
8 New Delhi 110003, India

9 ^c Department of Environment, Central Denmark Region, Lægårdvej 10, 7500 Holstebro,
10 Denmark

11 *Email: hans.richnow@ufz.de Tel: 0049 341 235 1212 Fax: 0341-450822

12 **Abstract**

13 The applicability of compound-specific isotope analysis (CSIA) for assessing *in situ* hydrolysis
14 of parathion was investigated in a contaminated aquifer at a former pesticide wastes landfill site.
15 Stable isotope analysis of parathion extracted from groundwater taken from different monitoring
16 wells revealed a maximum enrichment in carbon isotope ratio of +4.9 ‰ compared to the source
17 of parathion, providing evidence that *in situ* hydrolysis took place. Calculations based on the
18 Rayleigh-equation approach indicated that the natural attenuation of parathion was up to 8.6% by
19 hydrolysis under neutral and acidic conditions. In degradation experiments with aerobic and
20 anaerobic parathion-degrading microbes, no carbon and hydrogen isotope fractionation of
21 parathion were observed. For the first time, CSIA has been applied for the exclusive assessment

22 of the hydrolysis of phosphorothioate-containing organophosphorus pesticides at a contaminated
23 field site.

24 Key words: isotope fractionation, parathion, *in situ* hydrolysis, field application, CSIA

25 **1. Introduction**

26 Organophosphorus pesticides (OPs) have been used mainly as insecticides throughout the world
27 since the decline in the use of organochlorine pesticides in the 1960s and 1970s. OPs exhibit
28 acute toxicity by inhibiting acetylcholinesterase (AChE) in the nervous system. Today the
29 consumption of OPs ranks second relative to the total global pesticide usage (Fenner et al. 2013).
30 OPs are considered to be degradable in the environment in contrast to organochlorines, however,
31 continuous and excessive use of OPs has led to environmental contaminations which raise public
32 concerns (USEPA 2006) as the residues have repeatedly been detected in soils, sediments,
33 waterbodies, air samples, fishes and humans (Aston and Seiber 1996, Kawahara et al. 2005,
34 Pehkonen and Zhang 2002). Parathion (O,O-diethyl O-(4-nitrophenyl) phosphorothioate) was
35 one of the most widely used organophosphorus insecticides in agriculture in the past decades,
36 and was primarily used on fruit, cotton, wheat, vegetables, and nut crops (FAO 1990). Due to its
37 toxicity, parathion has been banned or restricted in many countries; however, stockpiles and
38 waste from previous manufacturing and former landfill sites often contain parathion (LRSB 2014,
39 Nielsen et al. 2014) forming serious point source contaminations which require management
40 strategies. Thus, it is important to understand the chemical fate of parathion for properly
41 environmental risks assessment at landfill sites and for groundwater quality protection and
42 management.

43 Hydrolysis is believed to be one of the major pathways controlling the fate of OPs in the
44 environment. Hydrolysis of OPs proceeds by a common mechanism, where H₂O and OH⁻ act as
45 nucleophiles in a bimolecular nucleophilic substitution mechanism (S_N2 mechanism) (Pehkonen
46 and Zhang 2002, Thatcher and Kluger 1989). The ester bonds of OPs can be hydrolyzed under
47 acidic and alkaline conditions by two different pathways whereas the relative contribution of
48 each hydrolysis pathway is pH-dependent (Wu et al. 2018). Alkaline hydrolysis is much faster
49 compared to acidic and neutral hydrolysis. For example, the half-life of parathion is reported to
50 be 133 days at pH 5 (25 °C), 247 days at pH 7 (25 °C), 102 days at pH 9 (25 °C) (FAO 1990),
51 and only 1.14 days at pH 12 (20 °C) (Wu et al. 2018). Generally, alkaline hydrolysis is unlikely
52 to contribute significantly to the natural attenuation of parathion, since mostly neutral and
53 slightly acidic conditions prevailing in the environment. Therefore, hydrolysis under neutral or
54 slightly acidic environmental conditions will lead to long half-life of parathion. The pH of
55 seawater is typically limited to a range between 7.5 and 8.4 and seawater intrusions in
56 dumpsites affected by tidal fluctuation may potentially contribute to increase *in situ* hydrolysis.

57 Compound specific isotope analysis (CSIA) opens the door to the development of field-based
58 assessment of degradation reactions. CSIA is one of the most promising fate investigative tools
59 which enable the detection of *in situ* biodegradation of organic contaminants (Nijenhuis and
60 Richnow 2016, Vogt et al. 2016). It has been used to estimate the extent of biodegradation of a
61 specific compound from changes in isotope ratios of field samples if the isotope enrichment
62 factor (ε) of that compound is determined in laboratory experiments based on the Rayleigh
63 equation (Bashir et al. 2015, Hofstetter et al. 2008, Liu et al. 2017, Thullner et al. 2012). The
64 molecular size of many micropollutants, such as pesticides, consumer care products or
65 pharmaceuticals, is greater than of typical legacy contaminants (chlorinated-compounds, benzene,

66 and toluene) thus limiting the sensitivity of CSIA. As only bond change reactions induce kinetic
67 isotope effects used for charactering degradation reactions, large molecules exhibit more atoms
68 which are not reacting. Thus, changes in single element isotope ratios (e.g. $\delta^{13}\text{C}$) tend to
69 become smaller with larger molecular size due to isotope dilution effects of non-reacting atoms.
70 Moreover, single element isotope ratios in the field can be always influenced by masking of
71 isotope fractionation which makes the identification of degradation pathways by single element
72 isotope analysis more difficult (Elsner 2010). Multi-element isotope analysis offers an
73 opportunity to circumvent the problem associated with single-element CSIA as it allows
74 characterizing bond change reactions of several elements.

75 In previous studies, we analyzed the carbon and hydrogen isotope fractionation of several OPs
76 upon chemical oxidation and hydrolysis in laboratory experiments (Wu et al. 2018, Wu et al.
77 2014). We could show that the rate-limiting step of the UV/H₂O₂ reaction of parathion is the
78 oxidative attack of the OH radical on the P=S bond, as indicated by negligible carbon and
79 hydrogen isotope fractionation. The hydrolysis of parathion under acidic and alkaline conditions
80 resulted in distinct but different carbon isotope fractionation patterns, principally allowing the
81 distinction of the two different pH-dependent pathways and giving the possibility for
82 characterizing natural attenuation of parathion by hydrolysis in the environment using isotope
83 fractionation concepts.

84 CSIA has been widely used for biodegradation assessment of different contaminant groups
85 (Elsner 2010, Thullner et al. 2012). Recently Vogt and colleges summarized the concepts for
86 applying CSIA for characterization of natural attenuation of hydrocarbons in field studies (Vogt
87 et al. 2016). In addition, CSIA has been proposed as a useful approach for characterizing
88 degradation processes of micropollutants such as pesticides at field scale (Elsner and Imfeld

89 2016); however, only in a few field studies CSIA has been applied to assess microbial
90 degradation of different pesticides or herbicides (Bashir et al. 2015, Liu et al. 2017, Milosevic et
91 al. 2013). To our best knowledge, CSIA has not yet been applied in field studies to assess the *in*
92 *situ* degradation of OPs. In order to fill this research gap, we selected parathion as a model
93 compound of OPs and investigated its natural attenuation by hydrolysis at a contaminated site
94 using carbon and hydrogen isotope analysis.

95 **2. Materials and methods**

96 **2.1. Chemicals**

97 Parathion (*O,O*-diethyl *O*-(4-nitrophenyl) phosphorothioate, >99.7%) was purchased from
98 Sigma-Aldrich and dichloromethane (DCM, $\geq 99.9\%$) was from Carl Roth GmbH & Co. KG,
99 Germany. Anhydrous Na₂SO₄ ($\geq 99\%$) was obtained from Bernd Kraft GmbH, Germany.

100 **2.2. Field site and sampling**

101 Groyne 42 is situated at Harboøre Tongue in Denmark facing the North Sea. Between 1950 and
102 1960, waste chemicals were disposed at the site. The area is still heavily contaminated by
103 approximately 100 tons of primarily OPs, mainly the highly toxic parathion (NorthPestClean
104 2014a). A complex dense non-aqueous phase liquid (DNAPL) presenting in Groyne 42 is a
105 mixture of OPs and intermediate products, reactants, and solvents used or produced in the
106 manufacturing of OPs. The background information of this site has been described elsewhere
107 (Bondgaard et al. 2012, Hvidberg et al. 2008). In 2006 the contaminated area (20,000 m²) was
108 encapsulated by installing a 600 m long and 14 m deep steel sheet piling and a plastic membrane
109 cap in order to prevent further leaching of toxins to the seawater (Fig. S1, (NorthPestClean
110 2014a)). From 2007 to 2014 the Central Denmark Region and the Danish Environmental

111 Protection Agency conducted research to develop a new *in situ* treatment of the site. The
112 treatment consisted of *in situ* alkaline hydrolysis (ISAH) combined with pump-and-treat. The
113 demonstration experiments were carried out on site in controlled test cells (TCs) and test pipes
114 (TPs). More information can be found in the online reports from North Pest Clean
115 (NorthPestClean). Because of the demonstration experiments in the NorthPestClean project, the
116 site contained discrete areas which are the treated areas with sodium hydroxide (pH 13) and the
117 untreated areas with neutral to acidic conditions (pH 2-7). By 2014, the total removal of
118 contaminants from TCs and TPs in treated areas is up to 85% from water and 76% from
119 sediment by ISAH combined with pump-and-treat (NorthPestClean 2014b). However, the natural
120 attenuation of parathion in the untreated area remains unknown due to the lack of efficient
121 assessment methods.

122 The locations of monitoring wells are indicated in Fig. 1. Two free phase samples from the
123 Groyne 42 DNAPL were taken in 2011 and 2014 and used to characterize the isotopic
124 composition of the source of parathion. The Groyne 42 DNAPL has a density of 1.16 g mL⁻¹ and
125 viscosity of 13.9 cP at 10 °C (Muff et al. 2016). The composition by weight of the DNAPL was
126 characterized to be 62 % parathion, 9 % methyl-parathion (*O,O*-dimethyl-*O-p*-
127 nitrophenylphosphorothioate), 7 % mercury, 5 % sulfotep (diethoxyphosphinothioxyloxy-
128 diethoxy-sulfanylidene- λ 5-phosphane), 3 % malathion (diethyl 2-
129 [(dimethoxyphosphorothioyl)sulfanyl]butanedioate) and 14 % other unknown contaminants
130 (NorthPestClean 2014a). The free phase samples were dissolved in DCM and directly subjected
131 for carbon and hydrogen isotope analysis to be used as the source signature of parathion.

132 19 samples were collected from monitoring wells installed in the treated area and 17 samples
133 were collected from the untreated area using a submersible electrical pump. 1 L of brown glass

134 bottles (Schott, Germany) were used for sampling from the treated area where high
135 concentrations of parathion were expected. In order to avoid evaporation of parathion, bottles
136 were filled with groundwater almost completely and sealed with Teflon-coated caps (Schott,
137 Germany) without headspace. The pH of groundwater samples was adjusted to neutral or slightly
138 acidic conditions using 25 % HCl solution (Carl Roth GmbH & Co. KG, Germany) to inhibit
139 alkaline hydrolysis. Neutralization was monitored by universal pH indicator strips (0-14 pH
140 Indicator Strips, Macherey-Nagel). 2.5 L of brown glass bottles (Schott, Germany) were used for
141 sampling from the untreated area using the same procedures as described above but without
142 adjusting the pH, because parathion has a relative slow hydrolysis rate at neutral to acidic
143 conditions. The ground water level was measured on-site by an EL-WA water level meters. The
144 concentrations of dissolved oxygen, temperature, pH, and electrical conductivity (EC) were
145 measured on-site during sampling using a Multimeter (WTW, Weilheim, Germany). Samples
146 were sent to the laboratory and stored at 4 °C until extraction. The extraction of samples was
147 processed within 2 weeks after sampling.

148 **2.3. Sample preparation**

149 Groundwater samples were transferred into a 2 L glass-separation funnel. Each sample was
150 extracted three times with 100 mL, 50 mL, and 50 mL of DCM, respectively, by shaking
151 thoroughly. The organic phases were combined and evaporated to ~2 mL under a gentle stream
152 of N₂ in a TurboVap concentrator (TurboVap II, Biotage, Sweden). The extraction and
153 evaporation procedure did not result in significant changes in carbon and hydrogen isotope ratios
154 of parathion as shown elsewhere (Wu et al. 2017). The concentrated sample from the untreated
155 area was then transferred into a 4 mL glass vial by a glass pipette and reconstituted into 3 mL of
156 DCM. The concentrated sample from the treated area was transferred into a 20 mL glass vial by

157 a glass pipette and reconstituted into 10 mL of DCM due to the high concentration of parathion.
158 Before analysis approximately 1.5 g (untreated area) or 5 g (treated area) of anhydrous Na₂SO₄
159 were added in each vial to remove water.

160 **2.4. Aerobic and anaerobic degradation of parathion**

161 In order to investigate the isotopic profiles of parathion during biodegradation, experiments were
162 conducted using two isolated aerobic strains (TERI OP1, TERI OP2) and one anaerobic strain
163 (TERI ANA-1), respectively. The strains were isolated from soil samples collected from nearby
164 garden located in Gwal Pahari (Gurgaon, Haryana), India. The aerobic strains were isolated in
165 mineral salt (MS) medium with compositions as described elsewhere (Rokade and Mali 2013).
166 Enrichment and isolation of anaerobic parathion degraders was carried out under strictly anoxic
167 conditions. MS medium was prepared under anaerobic condition as described elsewhere
168 (Junghare et al. 2012), by simultaneous boiling for 10 min and purging with nitrogen flush to
169 remove the dissolved oxygen. 0.1% of resazurin was added as redox indicator and L-cysteine
170 HCL (2.5 %) was added as a reducing agent to maintain the anoxic conditions. More details of
171 the enrichment and isolation of strains were described in the Supporting Information (section 3.1,
172 3.2 and 4.1). Batch experiments were conducted under oxic and anoxic conditions in 500 mL
173 flasks containing 250 mL MS medium for studying parathion degradation kinetics. For each
174 batch experiment, seven flasks containing 34 µM parathion-spiked MS medium were inoculated
175 with 1 mL of inoculum. More information about inoculum preparation is provided in the
176 Supporting Information (section 3.3). Sterile control flasks were prepared by the same
177 procedures except adding inoculum. All control and culture flasks were incubated at 150 rpm
178 and 30 °C in the dark. At different time intervals, 1 mL culture broth was taken for optical
179 density and pH variation measurement. Residual parathion and potential metabolites in the

180 medium were extracted by 10 mL of DCM containing naphthalene (6.5 mg L^{-1}) as internal
181 standard for further analysis.

182 **2.5. Analytical methods and quantification.**

183 **2.5.1. Concentration measurement.**

184 Parathion was quantified using an Agilent 6890 series GC (Agilent Technologies, USA)
185 equipped with a flame ionization detector (FID) as described elsewhere (Wu et al. 2018, Wu et al.
186 2017). A modified temperature program was used: the column was initially held at $60 \text{ }^\circ\text{C}$ for 2
187 min, and increased at $8 \text{ }^\circ\text{C min}^{-1}$ to $280 \text{ }^\circ\text{C}$, and then held for 2 min.

188 **2.5.2. Isotope analysis.**

189 The carbon isotope compositions of parathion were analyzed by a gas chromatography-
190 combustion-isotope ratio mass spectrometer (GC-C-IRMS) system, which consists of a GC
191 7890A (Agilent Technologies, Palo Alto, CA, USA) coupled via a ConFlo IV interface (Thermo
192 Fisher Scientific, Germany) to a MAT 253 IRMS (Thermo Fisher Scientific, Germany) via an
193 open split. High-temperature pyrolysis was used to convert organically bound hydrogen into
194 molecular hydrogen at $1200 \text{ }^\circ\text{C}$ for hydrogen isotope composition measurement via the gas
195 chromatograph- high temperature conversion-isotope ratio mass spectrometer system (GC-HTC-
196 IRMS). A DB-608 column ($30 \text{ m} \times 0.32 \text{ mm} \times 0.5 \text{ } \mu\text{m}$, Agilent J&W, USA) was used for sample
197 separation, the column was initially held at $60 \text{ }^\circ\text{C}$ for 2 min, and increased at $8 \text{ }^\circ\text{C min}^{-1}$ to
198 $280 \text{ }^\circ\text{C}$, and then held for 2 min. All samples were measured in triplicate. The other analytical
199 details are the same as described elsewhere (Wu et al. 2017).

200 **2.5.3. Quantification of parathion degradation in the field**

201 The carbon and hydrogen isotopic signatures are reported as δ values in parts per thousand (‰)
202 relative to international reference materials which are Vienna PeeDee Belemnite (VPDB) for
203 carbon and Standard Mean Ocean Water (SMOW) for hydrogen (Coplen 2011, Coplen et al.
204 2006, Schimmelmann et al. 2016). A main objective of CSIA is to quantify the amount of
205 (chemical or biological) degradation in the field supporting monitored natural attenuation (MNA)
206 as a site remedy. The extent of degradation can be estimated for individual compounds using the
207 isotope shifts between the source and the residual not yet degraded fraction of the reacting
208 compound using the Eq. (1) which is derived from the rearrangement of the logarithmic form of
209 the Rayleigh equation Eq. (2) (Meckenstock et al. 2004):

$$210 \quad D (\%) = \left(1 - \frac{C_t}{C_0}\right) \times 100 = \left[1 - \left(\frac{\delta_t + 1}{\delta_0 + 1}\right)^{\left(\frac{1}{\varepsilon}\right)}\right] \times 100 \quad (1)$$

$$211 \quad \ln\left(\frac{\delta_t + 1}{\delta_0 + 1}\right) = \varepsilon \times \ln\left(\frac{C_t}{C_0}\right) \quad (2)$$

212 where C_t is the concentration at a given reaction time t or on a flow path downgradient a source;
213 C_0 is the concentration at the beginning of a reaction or in source area; δ_t and δ_0 are the
214 corresponding carbon and hydrogen isotope ratios of the reacting compound; ε is the isotope
215 enrichment factor for a degradation process, which can be obtained from reference experiment
216 under laboratory condition using Rayleigh equation Eq. (2). Thus, the extent of degradation ($D\%$)
217 in the field can be retrieved from isotope values alone, without additional information on
218 concentrations or transformation products.

219 **3. Results and discussion**

220 **3.1. Parathion distribution and hydrogeochemical conditions**

221 The physicochemical parameters of the groundwater samples are listed in Table 1. The
222 groundwater level in the monitoring wells ranged from 1.40 to 5.15 m below surface. The
223 temperature was between 11.4 and 13.0 °C. Concentrations of dissolved oxygen were always
224 below 0.1 mg L⁻¹, indicating almost anoxic conditions. In the untreated area, the pH ranged from
225 3.2 to 6.5, the acidic conditions were likely due to acid chemical waste deposition. Only one well
226 in this area showed an alkaline pH of 9.4 (well V03-2). Parathion concentrations of samples from
227 the untreated area were always lower than 5 mg L⁻¹. In the treated area, the pH ranged from 6.9
228 to 12.4, demonstrating the effectiveness of the remediation measure. Samples from well TC3-9-3
229 in the treated area were strongly acidic (pH 2.2) indicating that this well is very close to the core
230 of acid waste deposition and mixing of alkaline solutions with DNAPL did not result in alkaline
231 conditions. The concentrations of parathion varied from 0.76 to 155.33 mg L⁻¹ in the wells within
232 the treated area (Table 1). The solubility of parathion is 10.4 mg L⁻¹ in water at 8 °C (the average
233 temperature of ground water in Denmark), which is calculated using the enthalpy of fusion for
234 parathion as described elsewhere (Polatoğlu et al. 2015). Most of the parathion concentrations
235 levels in the treated area are above its solubility. This is due to that the treated area is located at
236 the contamination hotspot (Fig. 1) where free organic phases of a mixture of OPs, intermediate
237 products, reactants, as well as solvents used in the manufacturing of OPs are present. Free
238 contaminant phases probably fill pore space of the sediment implying a limited contact to water
239 phases, thus reducing the mixing with alkaline water in the treated area. The large variations of
240 pH values and parathion concentrations in both areas illustrate rather heterogenic
241 biogeochemical conditions at the investigated site.

242 Potential transformation products of parathion were investigated in different treated and
243 untreated areas of the site (Fig. S2 and Table S1). The relative abundance and frequency of

244 detected aminoparathion (4-diethoxyphosphinothioxyloxyaniline) suggested reduction of the nitro
245 group of parathion by chemical or microbial processes (see also below). Compared to the treated
246 area, the higher abundance of aminoparathion in the untreated area (Table S1) showing neutral
247 and acidic conditions indicates that the reduction of the nitro group is preferentially a biological
248 process. The presence of aminoparathion may point to reducing conditions prevailing at the
249 dumpsite. Aminoparathion was detected in our biological degradation experiments under
250 aerobic conditions using strain TERI OP1 and under anoxic conditions using strain TERI ANA-1
251 as described below in section 3.4, which is also in line with previous studies (Singh and Walker
252 2006). *p*-nitrophenol (4-nitrophenol) is a typical alkaline hydrolysis product of parathion and was
253 detected in both untreated and treated areas. The relative abundance and detection frequency
254 were higher in the treated area (Table S1), showing the hydrolytic cleavage of the O-P bond. The
255 abundance of *p*-nitrophenol in biodegradation studies suggests that biological hydrolysis
256 potentially may contribute to transformation of parathion.

257 **3.2. Carbon and hydrogen isotope analysis of parathion from field samples**

258 The average value of all isotope analyses of source samples was taken as source signature of
259 parathion, resulting in -22.9 ± 0.8 ‰ for $\delta^{13}\text{C}$ (n = 10) and -212 ± 15 ‰ for $\delta^2\text{H}$ (n = 12). In the
260 untreated area, the obtained $\delta^{13}\text{C}$ values differed from -22.1 ‰ to -18.0 ‰ and $\delta^2\text{H}$ values
261 differed from -226 ‰ to -208 ‰ (Table 1). In the treated area, the $\delta^{13}\text{C}$ values varied from -23.6 ‰
262 to 20.1 ‰ and $\delta^2\text{H}$ values varied from -227 ‰ to -201 ‰ (Table 1).

263 Compared to the source signature of parathion, the $\delta^{13}\text{C}$ enrichment of 0.8 ‰ to 4.9 ‰ was
264 obtained from the wells in the untreated area (Fig. 2a), indicating *in situ* acidic and neutral
265 hydrolysis was taking place. In the treated area, the $\delta^{13}\text{C}$ values were almost identical with the

266 source signature (Fig. 2a) showing that no carbon isotope fractionation of parathion occurs
267 under strong alkaline conditions, which is in agreement with the results of laboratory hydrolysis
268 experiments (Wu et al. 2018). $\delta^{13}\text{C}$ enrichments of 2.8 ‰ and 2.1 ‰ were observed in samples
269 from wells TC3-6-3 and TC3-7-2, respectively, which are characterized by strongly alkaline pH
270 values (11.7 -12.4). This result might be explained by mixing of alkaline water and plumes
271 during sampling. Mixing of water in porous media under laminar flow conditions in sandy
272 aquifers is restricted, which imply that alkaline solution will not mix easily with contaminant
273 phases or highly contaminated water. Mass transfer processes are widely controlled by diffusive
274 transport resulting in transversal dispersion along a flow path. Convective mixing in porous
275 sediments practically can be neglected. For example mixing of contaminants with electron donor
276 or acceptor under laminar flow conditions can be limiting for biodegradation. Mixing during
277 sampling need to be taken into account for interpreting isotope composition and lead to an
278 underestimation of degradation reactions (Kopinke et al. 2005). Mixing of water bodies from
279 different section of an aquifer with specific reaction conditions should be considered for
280 quantitative interpretation of isotope fractionation pattern (Thullner et al. 2012). The isotope
281 fractionation is an indication that the hydrolysis may have taken place under acidic, neutral or
282 slight alkaline conditions explaining the carbon isotope enrichment. However, in both treated and
283 untreated areas, the $\delta^2\text{H}$ values were all overlapping with the source signature (Fig. 2b) because
284 the hydrolysis of parathion is not associated to a detectable hydrogen isotope fractionation effect,
285 independent of the pH value.

286 **3.3. Isotopic profiles of parathion during hydrolysis and chemical oxidation**

287 Carbon and hydrogen isotope fractionation patterns of hydrolysis and chemical oxidation of
288 parathion have been investigated systematically in our previous study (Wu et al. 2018). Chemical

289 oxidation of parathion occurs via oxidation of the P=S bond to a P=O bond by an OH radical in
290 the first rate-determining irreversible step (Fig. 3B); the reaction is not linked to detectable
291 hydrogen or carbon isotope fractionation. In contrast, the hydrolysis of parathion results in no
292 detectable H isotope fractionation but significant C isotope fractionation, corresponding to
293 isotope enrichment factors of $\epsilon_C = -6.9 \pm 0.8 \text{ ‰}$ at pH 2, $-6.7 \pm 0.4 \text{ ‰}$ at pH 5, $-6.0 \pm 0.2 \text{ ‰}$ at
294 pH 7, $-3.5 \pm 0.4 \text{ ‰}$ at pH 9, and no detectable carbon isotope fractionation at pH 12. The
295 different isotope fractionation patterns are due to two hydrolysis pathways of parathion (Fig. 3A):
296 one is P-O bond cleavage by nucleophilic attack at the phosphorus atom under strong alkaline
297 condition, resulting in no C and H isotope fractionation; another one is C-O bond cleavage by
298 nucleophilic attack at the carbon atom under acidic, neutral and slightly alkaline conditions,
299 resulting in a significant C but no H isotope fractionation.

300 The obtained ϵ_C at pH 2, pH5 and pH7 are identical when considering the confidence intervals.
301 This is due to the similar pathway takes place under neutral and acidic hydrolysis (Fig. 3A1)
302 which cannot be by isotope fractionation. In the case of lower pH < 7, the changes of pH have
303 effect on the reaction rates, for instance, the hydrolysis half-life of parathion at 25 °C is reported
304 to be 133 days at pH 5 and 247 days at pH 7 (FAO 1990). However, no effects of pH changes on
305 the reaction pathway and therefore the identical ϵ_C were obtained. Two hydrolysis pathways take
306 place simultaneously in the range of $7 < \text{pH} < 10$. With the increase of pH, the contribution from
307 C-O bond cleavage pathway decreases, resulting in smaller ϵ_C . The reduction of the ϵ_C at pH 9
308 revealed that the contribution to parathion degradation via C-O bond cleavage pathway is 51–58%
309 (Wu et al. 2018) using the extended Rayleigh-type equation derived by Van Breukelen (Van
310 Breukelen 2007). Parathion is hydrolyzed completely by the P-O bond cleavage pathway at pH >
311 10, as shown experimentally (Wanamaker et al. 2013), which is in agree with the result that no

312 detectable ϵ_C was obtained during hydrolysis at pH 12. Therefore, C isotope fractionation can be
313 expected and applied to characterize parathion hydrolysis at pH < 10.

314 **3.4. Isotopic profiles of parathion during biodegradation**

315 Isotopic profiles of parathion during biodegradation were investigated under laboratory
316 cultivation using two isolated aerobic strains (TERI OP1, TERI OP2) and one anaerobic strain
317 (TERI ANA-1). Experimental details with regard to the microbiological investigations are
318 described in the Supporting Information. During aerobic degradation of more than 80%
319 parathion, no carbon and hydrogen isotope enrichment could be observed (Table S2). Similarly
320 under anoxic conditions, no carbon and hydrogen isotope enrichment of parathion could be
321 observed after 90% degradation (Table S3). Thus, the reactions were not associated with carbon
322 and hydrogen isotope fractionation of parathion using the three tested strains. The potential
323 biodegradation metabolites of parathion were tentatively analyzed via GC-MS (for analytical
324 details see supporting information). The tentative metabolites analyses suggested that *p*-
325 nitrophenol, formed through the hydrolysis of the ester bond, was one initial reaction product
326 under aerobic conditions using strain TERI OP2. Aminoparathion was detected in degradation
327 experiments under aerobic conditions and anoxic conditions using strain TERI OP1 and strain
328 TERI ANA-1, respectively. This indicates that the biodegradation leads to the reduction of the
329 nitro group to form the amino group.

330 In previous studies, several microbial strains have been isolated capable of degrading parathion,
331 affiliated e.g. to the genera *Flavobacterium*, *Bacillus*, *Pseudomonas* or *Arthrobacter* (Singh and
332 Walker 2006). The previously proposed biodegradation mechanisms of parathion were
333 summarized in Fig. 3C, which are (C1) hydrolysis of the phosphotriester bond to form *p*-

334 nitrophenol (P-O bond cleavage), which is the major pathway; (C2) reduction of the nitro group
335 acting as electron acceptor to form aminoparathion (N-O bond cleavage); (C3) oxidation of the
336 sulfur group of parathion to form paraoxon (diethyl (4-nitrophenyl) phosphate) (P=S bond
337 cleavage). No carbon or hydrogen bonds breaking is involved in the first rate-determining
338 irreversible step of all three proposed pathways, thus, no significant carbon and/or hydrogen
339 isotope fractionation is expected to be associated with the biodegradation of parathion. Therefore,
340 the microbial degradation is not likely to be characterized by carbon and hydrogen isotope
341 fractionation. However, only a limited number of studies exist on aerobic and anaerobic
342 degradation of parathion, it cannot be fully excluded that microorganisms could attack parathion
343 by oxidizing a carbon entity leading to carbon and hydrogen isotope fractionation.

344 **3.5. Quantitative assessment of *in situ* hydrolysis at the investigated field site**

345 Even though the formation of OH radicals is unlikely in an anoxic or oxygen-limited aquifer, the
346 chemical oxidation of parathion leads to desulfurization in the rate-limiting step and would not
347 yield significant carbon or hydrogen isotope fractionation (Wu et al. 2018). As discussed above,
348 it is unlikely that significant carbon or hydrogen isotope fractionation is associated with the
349 biodegradation of parathion, and moreover, no carbon isotope fractionation can be expected
350 during the hydrolysis of parathion at pH > 10. Hence, the carbon isotope enrichment obtained in
351 parathion at the Groyne 42 site can be contributed exclusively to hydrolysis at pH < 10.

352 The extent of hydrolysis can be estimated by Eq. (1) using the ϵ_C determined in laboratory
353 experiments based on the Rayleigh equation. However, the accuracy of the degradation
354 estimation in the field is highly dependent on the choice of an appropriate ϵ_C for the given field
355 situation (USEPA 2008). The extent of *in situ* hydrolysis of parathion in the untreated area at the

356 Groyne 42 site was estimated using ϵ_C of -6.0 ± 0.2 (pH 7), -6.7 ± 0.4 (pH 5) and -6.9 ± 0.8 (pH
357 2), respectively. The estimation using carbon isotope enrichment revealed the evidence that up to
358 8.6 % natural attenuation of parathion was contributed by hydrolysis under neutral and acidic
359 conditions (Table 1). The ϵ_C of -3.5 ± 0.4 (pH 9) was used to estimate the extent of degradation
360 in the untreated area considering the mixed hydrolysis pathways, which resulted in up to 16 % of
361 natural attenuation of parathion was contributed by hydrolysis under slightly alkaline conditions
362 (Table 1). The low extent of *in situ* hydrolysis is due to long half-life of parathion under acidic
363 and neutral conditions and low ground water temperature at the field site (11-13 °C). The initial
364 concentration of parathion (C_0) in the untreated area was calculated by applying Eq. (1) using the
365 measured concentrations (C_t) and estimated extent of hydrolysis (Table 1). The initial
366 concentrations of parathion in monitored wells in the untreated area were calculated to be below
367 5.17 mg L^{-1} , which is below the solubility of 10.4 mg L^{-1} in water at 8 °C (the average
368 temperature of ground water in Denmark).

369 Muff and colleagues investigated the influence of co-solvents on the aqueous solubility and
370 reactivity of the OPs in the complex Groyne 42 DNAPL. Their results suggest that the hydrolysis
371 reactions are limited by the rate of hydrolysis rather than NAPL dissolution (Muff et al. 2016).
372 Chemical hydrolysis of parathion follows pseudo-first-order kinetics within the accuracy of
373 measurement. Half-life of the reactions conducted at pH 1 to 7.8 and temperatures from 0 to
374 90 °C under different conditions from different studies are summarized in Table S4. Arrhenius
375 plots are often used to analyze the effect of temperature on the rates of chemical reactions which
376 displays the logarithm of kinetic constants ($\ln(\kappa)$) plotted against inverse temperature ($1/T$). The
377 Arrhenius plot of parathion hydrolysis using collected data in Table S4 gave a straight line with
378 R^2 of 0.976 (Fig. 4), from which the activation energy (E_a) $92.04 \text{ kJ mol}^{-1}$ was determined. The

379 obtained E_a is in the same order of the previous reported value of $22.35 \text{ kcal mol}^{-1} = 93.52 \text{ kJ}$
380 mol^{-1} which was calculated from the hydrolysis of parathion at pH 7.8 at different temperatures
381 (Weber 1976). The equation obtained in Fig. 3 shows the correlation of temperature and the rate
382 constants of parathion hydrolysis at pH < 7.8. From this, a half-life of 1521 days at the average
383 ground water temperature in Denmark ($8 \text{ }^\circ\text{C}$) can be roughly predicted. The relative low
384 temperature at the Groyne 42 field site would lead to long retention time of parathion in the
385 untreated area. A previous study suggested that the enhancement of the average rate of
386 hydrolysis could be achieved by a factor of 1.4 - 4.8 by increasing reaction temperature from 10
387 to $30 \text{ }^\circ\text{C}$ (Muff et al. 2016). Our results contradicts to some extent with the assumption that the
388 rate of hydrolysis is the rate limiting step in the *in situ* degradation, and believe that mixing is a
389 major factor. Firstly, we found indication for neutral and acidic hydrolysis even in the treated
390 areas where someone would expect prevailing alkaline conditions. Secondly, the high parathion
391 concentrations clearly over the water solubility suggest that phases are present which are
392 obviously not assessable to hydrolysis. Thirdly, in spite of long half-life, the high concentrations
393 suggest that phases not assessable to hydrolysis still provide a source of contamination leaching
394 into the ground water.

395 Thus, the kinetic of hydrolytic transformation is expected to be controlled by mixing of alkaline
396 water in the subsurface, and mixing in porous media is slow. Similar assumption could be made
397 for neutral and acidic hydrolysis. Mixing of alkaline solutions with DNAPL seems to be a
398 challenge for all *in situ* measures. Heterogenic reaction conditions could be expected as
399 suggested by the carbon isotope enrichment of parathion even at places with high pH pointing to
400 a predominance of neutral or acidic hydrolysis.

401 **4. Conclusions**

402 Carbon isotope fractionation can be used to characterize acidic and neutral hydrolysis of
403 parathion at contaminated field sites. Anaerobic and aerobic biodegradation of parathion proceed
404 via reduction of the nitro group to aminoparathion and/or via enzymatic hydrolysis to *p*-
405 nitrophenol, and chemical oxidation by radicals occurs via desulfurization of parathion to
406 paraoxon; both reaction mechanisms were shown to be not associated with carbon and hydrogen
407 isotope fractionation. Therefore, the extent of hydrolysis under typical environmental pH values
408 (3-10) can be quantified robustly using the Rayleigh concept and the isotope enrichment factors
409 obtained in laboratory hydrolysis experiments.

410 At pH smaller than 7 where the C-O bond cleavage is the dominant hydrolysis pathway, the pH
411 changes will affect the reaction rate but has no effects on the carbon isotope enrichment factors
412 of parathion. In addition, hydrolysis rates increase with increasing temperature, for instance, the
413 half-life of parathion at pH 7 is 247 days at 25 °C (FAO 1990) and 75 hours at 60 °C (Wu et al.
414 2018). However, the mechanisms will not change and the isotope fractionation of S_N2 reaction is
415 considered to be not much effected by temperature. A previous study reported that the hydrolysis
416 rates of methyl halides increased with increasing temperature, while carbon kinetic isotope
417 effects for halide substitution were almost independent of temperature (Baesman and Miller
418 2005). This suggest that when both temperature and pH adjustments are required for technical
419 measures to improve parathion hydrolysis at contaminated sites, the isotope enrichment factors
420 obtained in laboratory hydrolysis experiments are still applicable to analyze the mode of
421 hydrolysis.

422 **Acknowledgment**

423 Langping Wu is financially supported by the China Scholarship Council (File No.
424 201306460007). The work was partially financially supported by BMBF-DBT Cooperation
425 Science Program (project No: 01DQ15006 and BT/IN/Germany-BMBF/02/BL/2015-16). We are
426 thankful to Steffen Kümmel and Matthias Gehre for support in the Isotope Laboratory of the
427 Department of Isotope Biogeochemistry.

428 Conflicts of interest: none

429 **References**

- 430 Aston, L.S. and Seiber, J.N. (1996) Exchange of airborne organophosphorus pesticides with pine
431 needles. *J. Environ. Sci. Heal. B* 31(4), 671-698.
- 432 Baesman, S.M. and Miller, L.G. (2005) Laboratory determination of the carbon kinetic isotope
433 effects (KIEs) for reactions of methyl halides with various nucleophiles in solution. *J. Atmos.*
434 *Chem.* 52(2), 203-219.
- 435 Bashir, S., Hitzfeld, K.L., Gehre, M., Richnow, H.H. and Fischer, A. (2015) Evaluating
436 degradation of hexachlorocyclohexane (HCH) isomers within a contaminated aquifer using
437 compound-specific stable carbon isotope analysis (CSIA). *Water Res.* 71, 187-196.
- 438 Bondgaard, M., Hvidberg, B. and Ramsay, L. (2012) Remediation of pesticide contamination by
439 in situ alkaline hydrolysis - a new soil remediation technology, Monterey, California.
- 440 Coplen, T.B. (2011) Guidelines and recommended terms for expression of stable-isotope-ratio
441 and gas-ratio measurement results. *Rapid Commun. Mass. Sp.* 25(17), 2538-2560.
- 442 Coplen, T.B., Brand, W.A., Gehre, M., Groning, M., Meijer, H.A.J., Toman, B. and Verkouteren,
443 R.M. (2006) After two decades a second anchor for the VPDB delta C-13 scale. *Rapid*
444 *Commun. Mass. Sp.* 20(21), 3165-3166.
- 445 Elsner, M. (2010) Stable isotope fractionation to investigate natural transformation mechanisms
446 of organic contaminants: principles, prospects and limitations. *J. Environ. Monit.* 12(11),
447 2005-2031.

448 Elsner, M. and Imfeld, G. (2016) Compound-specific isotope analysis (CSIA) of micropollutants
449 in the environment - current developments and future challenges. *Curr. Opin. Biotechnol.* 41,
450 60-72.

451 FAO (1990) Parathion (58), Food and Agriculture Organization of the United Nations.

452 Fenner, K., Canonica, S., Wackett, L.P. and Elsner, M. (2013) Evaluating pesticide degradation
453 in the environment: blind spots and emerging opportunities. *Science* 341(6147), 752-758.

454 Hofstetter, T.B., Schwarzenbach, R.P. and Bernasconi, S.M. (2008) Assessing transformation
455 processes of organic compounds using stable isotope fractionation. *Environ. Sci. Technol.*
456 42(21), 7737-7743.

457 Hvidberg, B., Ramsay, L., Kirkegaard, C., Elkjær, L., Jorgensen, C., Oberender, A. and Kiilerich,
458 O. (2008) Remediation technologies for a large pesticide-contaminated site: enclosure,
459 alkaline hydrolysis and bioventing.

460 Junghare, M., Subudhi, S. and B., L. (2012) Improvement of hydrogen production under
461 decreased partial pressure by newly isolated alkaline tolerated anaerobe, *Clostridium*
462 *butyricum* TM9A: optimization of process parameters. *Int. J. Hydrogen. Energ.* 4(37), 3160-
463 3168.

464 Kawahara, J., Horikoshi, R., Yamaguchi, T., Kumagai, K. and Yanagisawa, Y. (2005) Air
465 pollution and young children's inhalation exposure to organophosphorus pesticide in an
466 agricultural community in Japan. *Environ. Int.* 31(8), 1123-1132.

467 Kopinke, F.D., Georgi, A., Voskamp, M. and Richnow, H.H. (2005) Carbon isotope
468 fractionation of organic contaminants due to retardation on humic substances: Implications
469 for natural attenuation studies in aquifers. *Environ. Sci. Technol.* 39(16), 6052-6062.

470 Liu, Y., Bashir, S., Stollberg, R., Trabitsh, R., Weiss, H., Paschke, H., Nijenhuis, I. and
471 Richnow, H.H. (2017) Compound specific and enantioselective stable isotope analysis as
472 tools to monitor transformation of hexachlorocyclohexane (HCH) in a complex aquifer
473 System. *Environ. Sci. Technol.* 51(16), 8909-8916.

474 LRSB, L. (2014) Pilot experiments on the remediation technology in situ alkaline hydrolysis at
475 Groyne 42, Final report, NorthPestClean, Kongens Lyngby, Denmark.

476 Meckenstock, R.U., Morasch, B., Griebler, C. and Richnow, H.H. (2004) Stable isotope
477 fractionation analysis as a tool to monitor biodegradation in contaminated aquifers. *J.*
478 *Contam. Hydrol.* 75(3-4), 215-255.

479 Milosevic, N., Qiu, S., Elsner, M., Einsiedl, F., Maier, M.P., Bensch, H.K., Albrechtsen, H.J. and
480 Bjerg, P.L. (2013) Combined isotope and enantiomer analysis to assess the fate of phenoxy
481 acids in a heterogeneous geologic setting at an old landfill. *Water Res.* 47(2), 637-649.

482 Muff, J., MacKinnon, L., Durant, N.D., Bennedsen, L.F., Rugge, K., Bondgaard, M. and Pennell,
483 K. (2016) The influence of cosolvent and heat on the solubility and reactivity of
484 organophosphorous pesticide DNAPL alkaline hydrolysis. *Environ. Sci. Pollut. Res. Int.*
485 23(22), 22658-22666.

486 Nielsen, M.B., Kjeldsen, K.U., Lever, M.A. and Ingvorsen, K. (2014) Survival of prokaryotes in
487 a polluted waste dump during remediation by alkaline hydrolysis. *Ecotoxicology* 23, 404-
488 418.

489 Nijenhuis, I. and Richnow, H.H. (2016) Stable isotope fractionation concepts for characterizing
490 biotransformation of organohalides. *Curr. Opin. Biotechnol.* 41, 108-113.

491 NorthPestClean Projects related to the toxic waste site at Groyne 42
492 <http://www.eng.northpestclean.dk/publications/>.

493 NorthPestClean (2014a) Layman reports 2: Demonstration of in situ alkaline hydrolysis as a
494 novel soil remediation technique for a pesticide contamination, Central Denmark Region,
495 Department of Environment, <http://www.eng.northpestclean.dk/publications/layman-reports/>.

496 NorthPestClean (2014b) pilot experiments on the remediation technology in situ alkaline
497 hydrolysis at Groyne 42 - Final report,
498 [http://www.northpestclean.dk/publikationer/rapporter-fra-northpestclean-perioden-2011-
499 2014/](http://www.northpestclean.dk/publikationer/rapporter-fra-northpestclean-perioden-2011-2014/).

500 Pehkonen, S.O. and Zhang, Q. (2002) The degradation of organophosphorus pesticides in natural
501 waters: A critical review. *Crit. Rev. Env. Sci. Tec.* 32(1), 17-72.

502 Polatoğlu, İ., Yürekli, Y. and Baştürk, S.B. (2015) Estimating solubility of parathion in organic
503 solvents. *AKU J. Sci. Eng.* 15(3), 1-5.

504 Rokade, K.B. and Mali, G.V. (2013) Biodegradation of chlorpyrifos by *Pseudomonas*
505 *desmolyticum* NCIM 2112. *Int. J Pharm. Bio. Sci.* 2(4), (B) 609 - 616.

506 Schimmelmann, A., Qi, H.P., Coplen, T.B., Brand, W.A., Fong, J., Meier-Augenstein, W., Kemp,
507 H.F., Toman, B., Ackermann, A., Assonov, S., Aerts-Bijma, A.T., Brejcha, R., Chikaraishi,
508 Y., Darwish, T., Elsner, M., Gehre, M., Geilmann, H., Groing, M., Helie, J.F., Herrero-
509 Martin, S., Meijer, H.A.J., Sauer, P.E., Sessions, A.L. and Werner, R.A. (2016) Organic

510 reference materials for hydrogen, carbon, and nitrogen stable isotope-ratio measurements:
511 caffeines, n-alkanes, fatty acid methyl esters, glycines, L-valines, polyethylenes, and oils.
512 Anal. Chem. 88(8), 4294-4302.

513 Singh, B.K. and Walker, A. (2006) Microbial degradation of organophosphorus compounds.
514 Fems Microbiol. Rev. 30(3), 428-471.

515 Thatcher, G.R.J. and Kluger, R. (1989) Mechanism and catalysis of nucleophilic substitution in
516 phosphate esters. Adv. Phys. Org. Chem. 25, 99-265.

517 Thullner, M., Centler, F., Richnow, H.-H. and Fischer, A. (2012) Quantification of organic
518 pollutant degradation in contaminated aquifers using compound specific stable isotope
519 analysis – Review of recent developments. Org. Geochem. 42(12), 1440-1460.

520 USEPA (2006) Organophosphorus Cumulative Risk Assessment (2006 Update), pp. 1-189, U.S.
521 Environmental Protection Agency.

522 USEPA (2008) A guide for assessing biodegradation and source identification of organic ground
523 water contaminants using compound specific isotope analysis (CSIA). U.S. EPA Office of
524 Research and Development , N.R.M.R.L. (ed), p. 67, ADA OK.

525 Van Breukelen, B.M. (2007) Extending the Rayleigh equation to allow competing isotope
526 fractionating pathways to improve quantification of biodegradation. Environ. Sci. Technol.
527 41(11), 4004-4010.

528 Vogt, C., Dorer, C., Musat, F. and Richnow, H.H. (2016) Multi-element isotope fractionation
529 concepts to characterize the biodegradation of hydrocarbons - from enzymes to the
530 environment. Curr. Opin. Biotechnol. 41, 90-98.

531 Wanamaker, E.C., Chingas, G.C. and McDougal, O.M. (2013) Parathion hydrolysis revisited: in
532 situ aqueous kinetics by (1)h NMR. Environ. Sci. Technol. 47(16), 9267-9273.

533 Weber, K. (1976) Degradation of parathion in seawater. Water Res. 10(3), 237-241.

534 Wu, L., Chladkova, B., Lechtenfeld, O.J., Lian, S., Schindelka, J., Herrmann, H. and Richnow,
535 H.H. (2018) Characterizing chemical transformation of organophosphorus compounds by
536 (13)C and (2)H stable isotope analysis. Sci. Total. Environ. 615, 20-28.

537 Wu, L., Kummel, S. and Richnow, H.H. (2017) Validation of GC-IRMS techniques for delta C-
538 13 and delta H-2 CSIA of organophosphorus compounds and their potential for studying the
539 mode of hydrolysis in the environment. Anal. Bioanal. Chem. 409(10), 2581-2590.

540 Wu, L., Yao, J., Trebse, P., Zhang, N. and Richnow, H.H. (2014) Compound specific isotope
541 analysis of organophosphorus pesticides. *Chemosphere* 111, 458-463.

542

1 **Carbon and hydrogen isotope analysis of parathion for characterizing its natural**
2 **attenuation by hydrolysis at a contaminated site**

3 Langping Wu^a, Dipti Verma^b, Morten Bondgaard^c, Anja Melvej^c, Carsten Vogt^a, Sanjukta
4 Subudhi^b, Hans H. Richnow^{a,*}

5 ^a Department of Isotope Biogeochemistry, Helmholtz Centre for Environmental Research-UFZ,
6 Permoserstraße 15, 04318 Leipzig, Germany

7 ^b Environmental and Industrial Biotechnology Division, The Energy and Resources Institute,
8 New Delhi 110003, India

9 ^c Department of Environment, Central Denmark Region, Lægårdvej 10, 7500 Holstebro,
10 Denmark

11 *Email: hans.richnow@ufz.de Tel: 0049 341 235 1212 Fax: 0341-450822

12 **Abstract**

13 The applicability of compound-specific isotope analysis (CSIA) for assessing *in situ* hydrolysis
14 of parathion was investigated in a contaminated aquifer at a former pesticide wastes landfill site.
15 Stable isotope analysis of parathion extracted from groundwater taken from different monitoring
16 wells revealed a maximum enrichment in carbon isotope ratio of +4.9 ‰ compared to the source
17 of parathion, providing evidence that *in situ* hydrolysis took place. Calculations based on the
18 Rayleigh-equation approach indicated that the natural attenuation of parathion was up to 8.6% by
19 hydrolysis under neutral and acidic conditions. In degradation experiments with aerobic and
20 anaerobic parathion-degrading microbes, no carbon and hydrogen isotope fractionation of
21 parathion were observed. For the first time, CSIA has been applied for the exclusive assessment

22 of the hydrolysis of phosphorothioate-containing organophosphorus pesticides at a contaminated
23 field site.

24 Key words: isotope fractionation, parathion, *in situ* hydrolysis, field application, CSIA

25 **1. Introduction**

26 Organophosphorus pesticides (OPs) have been used mainly as insecticides throughout the world
27 since the decline in the use of organochlorine pesticides in the 1960s and 1970s. OPs exhibit
28 acute toxicity by inhibiting acetylcholinesterase (AChE) in the nervous system. Today the
29 consumption of OPs ranks second relative to the total global pesticide usage (Fenner et al. 2013).
30 OPs are considered to be degradable in the environment in contrast to organochlorines, however,
31 continuous and excessive use of OPs has led to environmental contaminations which raise public
32 concerns (USEPA 2006) as the residues have repeatedly been detected in soils, sediments,
33 waterbodies, air samples, fishes and humans (Aston and Seiber 1996, Kawahara et al. 2005,
34 Pehkonen and Zhang 2002). Parathion (O,O-diethyl O-(4-nitrophenyl) phosphorothioate) was
35 one of the most widely used organophosphorus insecticides in agriculture in the past decades,
36 and was primarily used on fruit, cotton, wheat, vegetables, and nut crops (FAO 1990). Due to its
37 toxicity, parathion has been banned or restricted in many countries; however, stockpiles and
38 waste from previous manufacturing and former landfill sites often contain parathion (LRSB 2014,
39 Nielsen et al. 2014) forming serious point source contaminations which require management
40 strategies. Thus, it is important to understand the chemical fate of parathion for properly
41 environmental risks assessment at landfill sites and for groundwater quality protection and
42 management.

43 Hydrolysis is believed to be one of the major pathways controlling the fate of OPs in the
44 environment. Hydrolysis of OPs proceeds by a common mechanism, where H₂O and OH⁻ act as
45 nucleophiles in a bimolecular nucleophilic substitution mechanism (S_N2 mechanism) (Pehkonen
46 and Zhang 2002, Thatcher and Kluger 1989). The ester bonds of OPs can be hydrolyzed under
47 acidic and alkaline conditions by two different pathways whereas the relative contribution of
48 each hydrolysis pathway is pH-dependent (Wu et al. 2018). Alkaline hydrolysis is much faster
49 compared to acidic and neutral hydrolysis. For example, the half-life of parathion is reported to
50 be 133 days at pH 5 (25 °C), 247 days at pH 7 (25 °C), 102 days at pH 9 (25 °C) (FAO 1990),
51 and only 1.14 days at pH 12 (20 °C) (Wu et al. 2018). Generally, alkaline hydrolysis is unlikely
52 to contribute significantly to the natural attenuation of parathion, since mostly neutral and
53 slightly acidic conditions prevailing in the environment. Therefore, hydrolysis under neutral or
54 slightly acidic environmental conditions will lead to long half-life of parathion. The pH of
55 seawater is typically limited to a range between 7.5 and 8.4 and seawater intrusions in
56 dumpsites affected by tidal fluctuation may potentially contribute to increase *in situ* hydrolysis.

57 Compound specific isotope analysis (CSIA) opens the door to the development of field-based
58 assessment of degradation reactions. CSIA is one of the most promising fate investigative tools
59 which enable the detection of *in situ* biodegradation of organic contaminants (Nijenhuis and
60 Richnow 2016, Vogt et al. 2016). It has been used to estimate the extent of biodegradation of a
61 specific compound from changes in isotope ratios of field samples if the isotope enrichment
62 factor (ϵ) of that compound is determined in laboratory experiments based on the Rayleigh
63 equation (Bashir et al. 2015, Hofstetter et al. 2008, Liu et al. 2017, Thullner et al. 2012). The
64 molecular size of many micropollutants, such as pesticides, consumer care products or
65 pharmaceuticals, is greater than of typical legacy contaminants (chlorinated-compounds, benzene,

66 and toluene) thus limiting the sensitivity of CSIA. As only bond change reactions induce kinetic
67 isotope effects used for charactering degradation reactions, large molecules exhibit more atoms
68 which are not reacting. Thus, changes in single element isotope ratios (e.g. $\delta^{13}\text{C}$) tend to
69 become smaller with larger molecular size due to isotope dilution effects of non-reacting atoms.
70 Moreover, single element isotope ratios in the field can be always influenced by masking of
71 isotope fractionation which makes the identification of degradation pathways by single element
72 isotope analysis more difficult (Elsner 2010). Multi-element isotope analysis offers an
73 opportunity to circumvent the problem associated with single-element CSIA as it allows
74 characterizing bond change reactions of several elements.

75 In previous studies, we analyzed the carbon and hydrogen isotope fractionation of several OPs
76 upon chemical oxidation and hydrolysis in laboratory experiments (Wu et al. 2018, Wu et al.
77 2014). We could show that the rate-limiting step of the UV/H₂O₂ reaction of parathion is the
78 oxidative attack of the OH radical on the P=S bond, as indicated by negligible carbon and
79 hydrogen isotope fractionation. The hydrolysis of parathion under acidic and alkaline conditions
80 resulted in distinct but different carbon isotope fractionation patterns, principally allowing the
81 distinction of the two different pH-dependent pathways and giving the possibility for
82 characterizing natural attenuation of parathion by hydrolysis in the environment using isotope
83 fractionation concepts.

84 CSIA has been widely used for biodegradation assessment of different contaminant groups
85 (Elsner 2010, Thullner et al. 2012). Recently Vogt and colleges summarized the concepts for
86 applying CSIA for characterization of natural attenuation of hydrocarbons in field studies (Vogt
87 et al. 2016). In addition, CSIA has been proposed as a useful approach for characterizing
88 degradation processes of micropollutants such as pesticides at field scale (Elsner and Imfeld

89 2016); however, only in a few field studies CSIA has been applied to assess microbial
90 degradation of different pesticides or herbicides (Bashir et al. 2015, Liu et al. 2017, Milosevic et
91 al. 2013). To our best knowledge, CSIA has not yet been applied in field studies to assess the *in*
92 *situ* degradation of OPs. In order to fill this research gap, we selected parathion as a model
93 compound of OPs and investigated its natural attenuation by hydrolysis at a contaminated site
94 using carbon and hydrogen isotope analysis.

95 **2. Materials and methods**

96 **2.1. Chemicals**

97 Parathion (*O,O*-diethyl *O*-(4-nitrophenyl) phosphorothioate, >99.7%) was purchased from
98 Sigma-Aldrich and dichloromethane (DCM, $\geq 99.9\%$) was from Carl Roth GmbH & Co. KG,
99 Germany. Anhydrous Na₂SO₄ ($\geq 99\%$) was obtained from Bernd Kraft GmbH, Germany.

100 **2.2. Field site and sampling**

101 Groyne 42 is situated at Harboøre Tongue in Denmark facing the North Sea. Between 1950 and
102 1960, waste chemicals were disposed at the site. The area is still heavily contaminated by
103 approximately 100 tons of primarily OPs, mainly the highly toxic parathion (NorthPestClean
104 2014a). A complex dense non-aqueous phase liquid (DNAPL) presenting in Groyne 42 is a
105 mixture of OPs and intermediate products, reactants, and solvents used or produced in the
106 manufacturing of OPs. The background information of this site has been described elsewhere
107 (Bondgaard et al. 2012, Hvidberg et al. 2008). In 2006 the contaminated area (20,000 m²) was
108 encapsulated by installing a 600 m long and 14 m deep steel sheet piling and a plastic membrane
109 cap in order to prevent further leaching of toxins to the seawater (Fig. S1, (NorthPestClean
110 2014a)). From 2007 to 2014 the Central Denmark Region and the Danish Environmental

111 Protection Agency conducted research to develop a new *in situ* treatment of the site. The
112 treatment consisted of *in situ* alkaline hydrolysis (ISAH) combined with pump-and-treat. The
113 demonstration experiments were carried out on site in controlled test cells (TCs) and test pipes
114 (TPs). More information can be found in the online reports from North Pest Clean
115 (NorthPestClean). Because of the demonstration experiments in the NorthPestClean project, the
116 site contained discrete areas which are the treated areas with sodium hydroxide (pH 13) and the
117 untreated areas with neutral to acidic conditions (pH 2-7). By 2014, the total removal of
118 contaminants from TCs and TPs in treated areas is up to 85% from water and 76% from
119 sediment by ISAH combined with pump-and-treat (NorthPestClean 2014b). However, the natural
120 attenuation of parathion in the untreated area remains unknown due to the lack of efficient
121 assessment methods.

122 The locations of monitoring wells are indicated in Fig. 1. Two free phase samples from the
123 Groyne 42 DNAPL were taken in 2011 and 2014 and used to characterize the isotopic
124 composition of the source of parathion. The Groyne 42 DNAPL has a density of 1.16 g mL⁻¹ and
125 viscosity of 13.9 cP at 10 °C (Muff et al. 2016). The composition by weight of the DNAPL was
126 characterized to be 62 % parathion, 9 % methyl-parathion (*O,O*-dimethyl-*O-p*-
127 nitrophenylphosphorothioate), 7 % mercury, 5 % sulfotep (diethoxyphosphinothioxyloxy-
128 diethoxy-sulfanylidene- λ 5-phosphane), 3 % malathion (diethyl 2-
129 [(dimethoxyphosphorothioyl)sulfanyl]butanedioate) and 14 % other unknown contaminants
130 (NorthPestClean 2014a). The free phase samples were dissolved in DCM and directly subjected
131 for carbon and hydrogen isotope analysis to be used as the source signature of parathion.

132 19 samples were collected from monitoring wells installed in the treated area and 17 samples
133 were collected from the untreated area using a submersible electrical pump. 1 L of brown glass

134 bottles (Schott, Germany) were used for sampling from the treated area where high
135 concentrations of parathion were expected. In order to avoid evaporation of parathion, bottles
136 were filled with groundwater almost completely and sealed with Teflon-coated caps (Schott,
137 Germany) without headspace. The pH of groundwater samples was adjusted to neutral or slightly
138 acidic conditions using 25 % HCl solution (Carl Roth GmbH & Co. KG, Germany) to inhibit
139 alkaline hydrolysis. Neutralization was monitored by universal pH indicator strips (0-14 pH
140 Indicator Strips, Macherey-Nagel). 2.5 L of brown glass bottles (Schott, Germany) were used for
141 sampling from the untreated area using the same procedures as described above but without
142 adjusting the pH, because parathion has a relative slow hydrolysis rate at neutral to acidic
143 conditions. The ground water level was measured on-site by an EL-WA water level meters. The
144 concentrations of dissolved oxygen, temperature, pH, and electrical conductivity (EC) were
145 measured on-site during sampling using a Multimeter (WTW, Weilheim, Germany). Samples
146 were sent to the laboratory and stored at 4 °C until extraction. The extraction of samples was
147 processed within 2 weeks after sampling.

148 **2.3. Sample preparation**

149 Groundwater samples were transferred into a 2 L glass-separation funnel. Each sample was
150 extracted three times with 100 mL, 50 mL, and 50 mL of DCM, respectively, by shaking
151 thoroughly. The organic phases were combined and evaporated to ~2 mL under a gentle stream
152 of N₂ in a TurboVap concentrator (TurboVap II, Biotage, Sweden). The extraction and
153 evaporation procedure did not result in significant changes in carbon and hydrogen isotope ratios
154 of parathion as shown elsewhere (Wu et al. 2017). The concentrated sample from the untreated
155 area was then transferred into a 4 mL glass vial by a glass pipette and reconstituted into 3 mL of
156 DCM. The concentrated sample from the treated area was transferred into a 20 mL glass vial by

157 a glass pipette and reconstituted into 10 mL of DCM due to the high concentration of parathion.
158 Before analysis approximately 1.5 g (untreated area) or 5 g (treated area) of anhydrous Na₂SO₄
159 were added in each vial to remove water.

160 **2.4. Aerobic and anaerobic degradation of parathion**

161 In order to investigate the isotopic profiles of parathion during biodegradation, experiments were
162 conducted using two isolated aerobic strains (TERI OP1, TERI OP2) and one anaerobic strain
163 (TERI ANA-1), respectively. The strains were isolated from soil samples collected from nearby
164 garden located in Gwal Pahari (Gurgaon, Haryana), India. The aerobic strains were isolated in
165 mineral salt (MS) medium with compositions as described elsewhere (Rokade and Mali 2013).
166 Enrichment and isolation of anaerobic parathion degraders was carried out under strictly anoxic
167 conditions. MS medium was prepared under anaerobic condition as described elsewhere
168 (Junghare et al. 2012), by simultaneous boiling for 10 min and purging with nitrogen flush to
169 remove the dissolved oxygen. 0.1% of resazurin was added as redox indicator and L-cysteine
170 HCL (2.5 %) was added as a reducing agent to maintain the anoxic conditions. More details of
171 the enrichment and isolation of strains were described in the Supporting Information (section 3.1,
172 3.2 and 4.1). Batch experiments were conducted under oxic and anoxic conditions in 500 mL
173 flasks containing 250 mL MS medium for studying parathion degradation kinetics. For each
174 batch experiment, seven flasks containing 34 µM parathion-spiked MS medium were inoculated
175 with 1 mL of inoculum. More information about inoculum preparation is provided in the
176 Supporting Information (section 3.3). Sterile control flasks were prepared by the same
177 procedures except adding inoculum. All control and culture flasks were incubated at 150 rpm
178 and 30 °C in the dark. At different time intervals, 1 mL culture broth was taken for optical
179 density and pH variation measurement. Residual parathion and potential metabolites in the

180 medium were extracted by 10 mL of DCM containing naphthalene (6.5 mg L^{-1}) as internal
181 standard for further analysis.

182 **2.5. Analytical methods and quantification.**

183 **2.5.1. Concentration measurement.**

184 Parathion was quantified using an Agilent 6890 series GC (Agilent Technologies, USA)
185 equipped with a flame ionization detector (FID) as described elsewhere (Wu et al. 2018, Wu et al.
186 2017). A modified temperature program was used: the column was initially held at $60 \text{ }^\circ\text{C}$ for 2
187 min, and increased at $8 \text{ }^\circ\text{C min}^{-1}$ to $280 \text{ }^\circ\text{C}$, and then held for 2 min.

188 **2.5.2. Isotope analysis.**

189 The carbon isotope compositions of parathion were analyzed by a gas chromatography-
190 combustion-isotope ratio mass spectrometer (GC-C-IRMS) system, which consists of a GC
191 7890A (Agilent Technologies, Palo Alto, CA, USA) coupled via a ConFlo IV interface (Thermo
192 Fisher Scientific, Germany) to a MAT 253 IRMS (Thermo Fisher Scientific, Germany) via an
193 open split. High-temperature pyrolysis was used to convert organically bound hydrogen into
194 molecular hydrogen at $1200 \text{ }^\circ\text{C}$ for hydrogen isotope composition measurement via the gas
195 chromatograph- high temperature conversion-isotope ratio mass spectrometer system (GC-HTC-
196 IRMS). A DB-608 column ($30 \text{ m} \times 0.32 \text{ mm} \times 0.5 \text{ } \mu\text{m}$, Agilent J&W, USA) was used for sample
197 separation, the column was initially held at $60 \text{ }^\circ\text{C}$ for 2 min, and increased at $8 \text{ }^\circ\text{C min}^{-1}$ to
198 $280 \text{ }^\circ\text{C}$, and then held for 2 min. All samples were measured in triplicate. The other analytical
199 details are the same as described elsewhere (Wu et al. 2017).

200 **2.5.3. Quantification of parathion degradation in the field**

201 The carbon and hydrogen isotopic signatures are reported as δ values in parts per thousand (‰)
202 relative to international reference materials which are Vienna PeeDee Belemnite (VPDB) for
203 carbon and Standard Mean Ocean Water (SMOW) for hydrogen (Coplen 2011, Coplen et al.
204 2006, Schimmelmann et al. 2016). A main objective of CSIA is to quantify the amount of
205 (chemical or biological) degradation in the field supporting monitored natural attenuation (MNA)
206 as a site remedy. The extent of degradation can be estimated for individual compounds using the
207 isotope shifts between the source and the residual not yet degraded fraction of the reacting
208 compound using the Eq. (1) which is derived from the rearrangement of the logarithmic form of
209 the Rayleigh equation Eq. (2) (Meckenstock et al. 2004):

$$210 \quad D (\%) = \left(1 - \frac{C_t}{C_0}\right) \times 100 = \left[1 - \left(\frac{\delta_t + 1}{\delta_0 + 1}\right)^{\left(\frac{1}{\varepsilon}\right)}\right] \times 100 \quad (1)$$

$$211 \quad \ln\left(\frac{\delta_t + 1}{\delta_0 + 1}\right) = \varepsilon \times \ln\left(\frac{C_t}{C_0}\right) \quad (2)$$

212 where C_t is the concentration at a given reaction time t or on a flow path downgradient a source;
213 C_0 is the concentration at the beginning of a reaction or in source area; δ_t and δ_0 are the
214 corresponding carbon and hydrogen isotope ratios of the reacting compound; ε is the isotope
215 enrichment factor for a degradation process, which can be obtained from reference experiment
216 under laboratory condition using Rayleigh equation Eq. (2). Thus, the extent of degradation ($D\%$)
217 in the field can be retrieved from isotope values alone, without additional information on
218 concentrations or transformation products.

219 **3. Results and discussion**

220 **3.1. Parathion distribution and hydrogeochemical conditions**

221 The physicochemical parameters of the groundwater samples are listed in Table 1. The
222 groundwater level in the monitoring wells ranged from 1.40 to 5.15 m below surface. The
223 temperature was between 11.4 and 13.0 °C. Concentrations of dissolved oxygen were always
224 below 0.1 mg L⁻¹, indicating almost anoxic conditions. In the untreated area, the pH ranged from
225 3.2 to 6.5, the acidic conditions were likely due to acid chemical waste deposition. Only one well
226 in this area showed an alkaline pH of 9.4 (well V03-2). Parathion concentrations of samples from
227 the untreated area were always lower than 5 mg L⁻¹. In the treated area, the pH ranged from 6.9
228 to 12.4, demonstrating the effectiveness of the remediation measure. Samples from well TC3-9-3
229 in the treated area were strongly acidic (pH 2.2) indicating that this well is very close to the core
230 of acid waste deposition and mixing of alkaline solutions with DNAPL did not result in alkaline
231 conditions. The concentrations of parathion varied from 0.76 to 155.33 mg L⁻¹ in the wells within
232 the treated area (Table 1). The solubility of parathion is 10.4 mg L⁻¹ in water at 8 °C (the average
233 temperature of ground water in Denmark), which is calculated using the enthalpy of fusion for
234 parathion as described elsewhere (Polatoğlu et al. 2015). Most of the parathion concentrations
235 levels in the treated area are above its solubility. This is due to that the treated area is located at
236 the contamination hotspot (Fig. 1) where free organic phases of a mixture of OPs, intermediate
237 products, reactants, as well as solvents used in the manufacturing of OPs are present. Free
238 contaminant phases probably fill pore space of the sediment implying a limited contact to water
239 phases, thus reducing the mixing with alkaline water in the treated area. The large variations of
240 pH values and parathion concentrations in both areas illustrate rather heterogenic
241 biogeochemical conditions at the investigated site.

242 Potential transformation products of parathion were investigated in different treated and
243 untreated areas of the site (Fig. S2 and Table S1). The relative abundance and frequency of

244 detected aminoparathion (4-diethoxyphosphinothioxyloxyaniline) suggested reduction of the nitro
245 group of parathion by chemical or microbial processes (see also below). Compared to the treated
246 area, the higher abundance of aminoparathion in the untreated area (Table S1) showing neutral
247 and acidic conditions indicates that the reduction of the nitro group is preferentially a biological
248 process. The presence of aminoparathion may point to reducing conditions prevailing at the
249 dumpsite. Aminoparathion was detected in our biological degradation experiments under
250 aerobic conditions using strain TERI OP1 and under anoxic conditions using strain TERI ANA-1
251 as described below in section 3.4, which is also in line with previous studies (Singh and Walker
252 2006). *p*-nitrophenol (4-nitrophenol) is a typical alkaline hydrolysis product of parathion and was
253 detected in both untreated and treated areas. The relative abundance and detection frequency
254 were higher in the treated area (Table S1), showing the hydrolytic cleavage of the O-P bond. The
255 abundance of *p*-nitrophenol in biodegradation studies suggests that biological hydrolysis
256 potentially may contribute to transformation of parathion.

257 **3.2. Carbon and hydrogen isotope analysis of parathion from field samples**

258 The average value of all isotope analyses of source samples was taken as source signature of
259 parathion, resulting in -22.9 ± 0.8 ‰ for $\delta^{13}\text{C}$ ($n = 10$) and -212 ± 15 ‰ for $\delta^2\text{H}$ ($n = 12$). In the
260 untreated area, the obtained $\delta^{13}\text{C}$ values differed from -22.1 ‰ to -18.0 ‰ and $\delta^2\text{H}$ values
261 differed from -226 ‰ to -208 ‰ (Table 1). In the treated area, the $\delta^{13}\text{C}$ values varied from -23.6 ‰
262 to 20.1 ‰ and $\delta^2\text{H}$ values varied from -227 ‰ to -201 ‰ (Table 1).

263 Compared to the source signature of parathion, the $\delta^{13}\text{C}$ enrichment of 0.8 ‰ to 4.9 ‰ was
264 obtained from the wells in the untreated area (Fig. 2a), indicating *in situ* acidic and neutral
265 hydrolysis was taking place. In the treated area, the $\delta^{13}\text{C}$ values were almost identical with the

266 source signature (Fig. 2a) showing that no carbon isotope fractionation of parathion occurs
267 under strong alkaline conditions, which is in agreement with the results of laboratory hydrolysis
268 experiments (Wu et al. 2018). $\delta^{13}\text{C}$ enrichments of 2.8 ‰ and 2.1 ‰ were observed in samples
269 from wells TC3-6-3 and TC3-7-2, respectively, which are characterized by strongly alkaline pH
270 values (11.7 -12.4). This result might be explained by mixing of alkaline water and plumes
271 during sampling. Mixing of water in porous media under laminar flow conditions in sandy
272 aquifers is restricted, which imply that alkaline solution will not mix easily with contaminant
273 phases or highly contaminated water. Mass transfer processes are widely controlled by diffusive
274 transport resulting in transversal dispersion along a flow path. Convective mixing in porous
275 sediments practically can be neglected. For example mixing of contaminants with electron donor
276 or acceptor under laminar flow conditions can be limiting for biodegradation. Mixing during
277 sampling need to be taken into account for interpreting isotope composition and lead to an
278 underestimation of degradation reactions (Kopinke et al. 2005). Mixing of water bodies from
279 different section of an aquifer with specific reaction conditions should be considered for
280 quantitative interpretation of isotope fractionation pattern (Thullner et al. 2012). The isotope
281 fractionation is an indication that the hydrolysis may have taken place under acidic, neutral or
282 slight alkaline conditions explaining the carbon isotope enrichment. However, in both treated and
283 untreated areas, the $\delta^2\text{H}$ values were all overlapping with the source signature (Fig. 2b) because
284 the hydrolysis of parathion is not associated to a detectable hydrogen isotope fractionation effect,
285 independent of the pH value.

286 **3.3. Isotopic profiles of parathion during hydrolysis and chemical oxidation**

287 Carbon and hydrogen isotope fractionation patterns of hydrolysis and chemical oxidation of
288 parathion have been investigated systematically in our previous study (Wu et al. 2018). Chemical

289 oxidation of parathion occurs via oxidation of the P=S bond to a P=O bond by an OH radical in
290 the first rate-determining irreversible step (Fig. 3B); the reaction is not linked to detectable
291 hydrogen or carbon isotope fractionation. In contrast, the hydrolysis of parathion results in no
292 detectable H isotope fractionation but significant C isotope fractionation, corresponding to
293 isotope enrichment factors of $\epsilon_C = -6.9 \pm 0.8 \text{ ‰}$ at pH 2, $-6.7 \pm 0.4 \text{ ‰}$ at pH 5, $-6.0 \pm 0.2 \text{ ‰}$ at
294 pH 7, $-3.5 \pm 0.4 \text{ ‰}$ at pH 9, and no detectable carbon isotope fractionation at pH 12. The
295 different isotope fractionation patterns are due to two hydrolysis pathways of parathion (Fig. 3A):
296 one is P-O bond cleavage by nucleophilic attack at the phosphorus atom under strong alkaline
297 condition, resulting in no C and H isotope fractionation; another one is C-O bond cleavage by
298 nucleophilic attack at the carbon atom under acidic, neutral and slightly alkaline conditions,
299 resulting in a significant C but no H isotope fractionation.

300 The obtained ϵ_C at pH 2, pH5 and pH7 are identical when considering the confidence intervals.
301 This is due to the similar pathway takes place under neutral and acidic hydrolysis (Fig. 3A1)
302 which cannot be by isotope fractionation. In the case of lower pH < 7, the changes of pH have
303 effect on the reaction rates, for instance, the hydrolysis half-life of parathion at 25 °C is reported
304 to be 133 days at pH 5 and 247 days at pH 7 (FAO 1990). However, no effects of pH changes on
305 the reaction pathway and therefore the identical ϵ_C were obtained. Two hydrolysis pathways take
306 place simultaneously in the range of $7 < \text{pH} > 10$. With the increase of pH, the contribution from
307 C-O bond cleavage pathway decreases, resulting in smaller ϵ_C . The reduction of the ϵ_C at pH 9
308 revealed that the contribution to parathion degradation via C-O bond cleavage pathway is 51–58%
309 (Wu et al. 2018) using the extended Rayleigh-type equation derived by Van Breukelen (Van
310 Breukelen 2007). Parathion is hydrolyzed completely by the P-O bond cleavage pathway at pH >
311 10, as shown experimentally (Wanamaker et al. 2013), which is in agree with the result that no

312 detectable ϵ_C was obtained during hydrolysis at pH 12. Therefore, C isotope fractionation can be
313 expected and applied to characterize parathion hydrolysis at pH < 10.

314 **3.4. Isotopic profiles of parathion during biodegradation**

315 Isotopic profiles of parathion during biodegradation were investigated under laboratory
316 cultivation using two isolated aerobic strains (TERI OP1, TERI OP2) and one anaerobic strain
317 (TERI ANA-1). Experimental details with regard to the microbiological investigations are
318 described in the Supporting Information. During aerobic degradation of more than 80%
319 parathion, no carbon and hydrogen isotope enrichment could be observed (Table S2). Similarly
320 under anoxic conditions, no carbon and hydrogen isotope enrichment of parathion could be
321 observed after 90% degradation (Table S3). Thus, the reactions were not associated with carbon
322 and hydrogen isotope fractionation of parathion using the three tested strains. The potential
323 biodegradation metabolites of parathion were tentatively analyzed via GC-MS (for analytical
324 details see supporting information). The tentative metabolites analyses suggested that *p*-
325 nitrophenol, formed through the hydrolysis of the ester bond, was one initial reaction product
326 under aerobic conditions using strain TERI OP2. Aminoparathion was detected in degradation
327 experiments under aerobic conditions and anoxic conditions using strain TERI OP1 and strain
328 TERI ANA-1, respectively. This indicates that the biodegradation leads to the reduction of the
329 nitro group to form the amino group.

330 In previous studies, several microbial strains have been isolated capable of degrading parathion,
331 affiliated e.g. to the genera *Flavobacterium*, *Bacillus*, *Pseudomonas* or *Arthrobacter* (Singh and
332 Walker 2006). The previously proposed biodegradation mechanisms of parathion were
333 summarized in Fig. 3C, which are (C1) hydrolysis of the phosphotriester bond to form *p*-

334 nitrophenol (P-O bond cleavage), which is the major pathway; (C2) reduction of the nitro group
335 acting as electron acceptor to form aminoparathion (N-O bond cleavage); (C3) oxidation of the
336 sulfur group of parathion to form paraoxon (diethyl (4-nitrophenyl) phosphate) (P=S bond
337 cleavage). No carbon or hydrogen bonds breaking is involved in the first rate-determining
338 irreversible step of all three proposed pathways, thus, no significant carbon and/or hydrogen
339 isotope fractionation is expected to be associated with the biodegradation of parathion. Therefore,
340 the microbial degradation is not likely to be characterized by carbon and hydrogen isotope
341 fractionation. However, only a limited number of studies exist on aerobic and anaerobic
342 degradation of parathion, it cannot be fully excluded that microorganisms could attack parathion
343 by oxidizing a carbon entity leading to carbon and hydrogen isotope fractionation.

344 **3.5. Quantitative assessment of *in situ* hydrolysis at the investigated field site**

345 Even though the formation of OH radicals is unlikely in an anoxic or oxygen-limited aquifer, the
346 chemical oxidation of parathion leads to desulfurization in the rate-limiting step and would not
347 yield significant carbon or hydrogen isotope fractionation (Wu et al. 2018). As discussed above,
348 it is unlikely that significant carbon or hydrogen isotope fractionation is associated with the
349 biodegradation of parathion, and moreover, no carbon isotope fractionation can be expected
350 during the hydrolysis of parathion at pH > 10. Hence, the carbon isotope enrichment obtained in
351 parathion at the Groyne 42 site can be contributed exclusively to hydrolysis at pH < 10.

352 The extent of hydrolysis can be estimated by Eq. (1) using the ϵ_C determined in laboratory
353 experiments based on the Rayleigh equation. However, the accuracy of the degradation
354 estimation in the field is highly dependent on the choice of an appropriate ϵ_C for the given field
355 situation (USEPA 2008). The extent of *in situ* hydrolysis of parathion in the untreated area at the

356 Groyne 42 site was estimated using ϵ_C of -6.0 ± 0.2 (pH 7), -6.7 ± 0.4 (pH 5) and -6.9 ± 0.8 (pH
357 2), respectively. The estimation using carbon isotope enrichment revealed the evidence that up to
358 8.6 % natural attenuation of parathion was contributed by hydrolysis under neutral and acidic
359 conditions (Table 1). The ϵ_C of -3.5 ± 0.4 (pH 9) was used to estimate the extent of degradation
360 in the untreated area considering the mixed hydrolysis pathways, which resulted in up to 16 % of
361 natural attenuation of parathion was contributed by hydrolysis under slightly alkaline conditions
362 (Table 1). The low extent of *in situ* hydrolysis is due to long half-life of parathion under acidic
363 and neutral conditions and low ground water temperature at the field site (11-13 °C). The initial
364 concentration of parathion (C_0) in the untreated area was calculated by applying Eq. (1) using the
365 measured concentrations (C_t) and estimated extent of hydrolysis (Table 1). The initial
366 concentrations of parathion in monitored wells in the untreated area were calculated to be below
367 5.17 mg L^{-1} , which is below the solubility of 10.4 mg L^{-1} in water at 8 °C (the average
368 temperature of ground water in Denmark).

369 Muff and colleagues investigated the influence of co-solvents on the aqueous solubility and
370 reactivity of the OPs in the complex Groyne 42 DNAPL. Their results suggest that the hydrolysis
371 reactions are limited by the rate of hydrolysis rather than NAPL dissolution (Muff et al. 2016).
372 Chemical hydrolysis of parathion follows pseudo-first-order kinetics within the accuracy of
373 measurement. Half-life of the reactions conducted at pH 1 to 7.8 and temperatures from 0 to
374 90 °C under different conditions from different studies are summarized in Table S4. Arrhenius
375 plots are often used to analyze the effect of temperature on the rates of chemical reactions which
376 displays the logarithm of kinetic constants ($\ln(\kappa)$) plotted against inverse temperature ($1/T$). The
377 Arrhenius plot of parathion hydrolysis using collected data in Table S4 gave a straight line with
378 R^2 of 0.976 (Fig. 4), from which the activation energy (E_a) $92.04 \text{ kJ mol}^{-1}$ was determined. The

379 obtained E_a is in the same order of the previous reported value of $22.35 \text{ kcal mol}^{-1} = 93.52 \text{ kJ}$
380 mol^{-1} which was calculated from the hydrolysis of parathion at pH 7.8 at different temperatures
381 (Weber 1976). The equation obtained in Fig. 3 shows the correlation of temperature and the rate
382 constants of parathion hydrolysis at pH < 7.8. From this, a half-life of 1521 days at the average
383 ground water temperature in Denmark ($8 \text{ }^\circ\text{C}$) can be roughly predicted. The relative low
384 temperature at the Groyne 42 field site would lead to long retention time of parathion in the
385 untreated area. A previous study suggested that the enhancement of the average rate of
386 hydrolysis could be achieved by a factor of 1.4 - 4.8 by increasing reaction temperature from 10
387 to $30 \text{ }^\circ\text{C}$ (Muff et al. 2016). Our results contradicts to some extent with the assumption that the
388 rate of hydrolysis is the rate limiting step in the *in situ* degradation, and believe that mixing is a
389 major factor. Firstly, we found indication for neutral and acidic hydrolysis even in the treated
390 areas where someone would expect prevailing alkaline conditions. Secondly, the high parathion
391 concentrations clearly over the water solubility suggest that phases are present which are
392 obviously not assessable to hydrolysis. Thirdly, in spite of long half-life, the high concentrations
393 suggest that phases not assessable to hydrolysis still provide a source of contamination leaching
394 into the ground water.

395 Thus, the kinetic of hydrolytic transformation is expected to be controlled by mixing of alkaline
396 water in the subsurface, and mixing in porous media is slow. Similar assumption could be made
397 for neutral and acidic hydrolysis. Mixing of alkaline solutions with DNAPL seems to be a
398 challenge for all *in situ* measures. Heterogenic reaction conditions could be expected as
399 suggested by the carbon isotope enrichment of parathion even at places with high pH pointing to
400 a predominance of neutral or acidic hydrolysis.

401 **4. Conclusions**

402 Carbon isotope fractionation can be used to characterize acidic and neutral hydrolysis of
403 parathion at contaminated field sites. Anaerobic and aerobic biodegradation of parathion proceed
404 via reduction of the nitro group to aminoparathion and/or via enzymatic hydrolysis to *p*-
405 nitrophenol, and chemical oxidation by radicals occurs via desulfurization of parathion to
406 paraoxon; both reaction mechanisms were shown to be not associated with carbon and hydrogen
407 isotope fractionation. Therefore, the extent of hydrolysis under typical environmental pH values
408 (3-10) can be quantified robustly using the Rayleigh concept and the isotope enrichment factors
409 obtained in laboratory hydrolysis experiments.

410 At pH smaller than 7 where the C-O bond cleavage is the dominant hydrolysis pathway, the pH
411 changes will affect the reaction rate but has no effects on the carbon isotope enrichment factors
412 of parathion. In addition, hydrolysis rates increase with increasing temperature, for instance, the
413 half-life of parathion at pH 7 is 247 days at 25 °C (FAO 1990) and 75 hours at 60 °C (Wu et al.
414 2018). However, the mechanisms will not change and the isotope fractionation of S_N2 reaction is
415 considered to be not much effected by temperature. A previous study reported that the hydrolysis
416 rates of methyl halides increased with increasing temperature, while carbon kinetic isotope
417 effects for halide substitution were almost independent of temperature (Baesman and Miller
418 2005). This suggest that when both temperature and pH adjustments are required for technical
419 measures to improve parathion hydrolysis at contaminated sites, the isotope enrichment factors
420 obtained in laboratory hydrolysis experiments are still applicable to analyze the mode of
421 hydrolysis.

422 **Acknowledgment**

423 Langping Wu is financially supported by the China Scholarship Council (File No.
424 201306460007). The work was partially financially supported by BMBF-DBT Cooperation
425 Science Program (project No: 01DQ15006 and BT/IN/Germany-BMBF/02/BL/2015-16). We are
426 thankful to Steffen Kümmel and Matthias Gehre for support in the Isotope Laboratory of the
427 Department of Isotope Biogeochemistry.

428 Conflicts of interest: none

429 **References**

- 430 Aston, L.S. and Seiber, J.N. (1996) Exchange of airborne organophosphorus pesticides with pine
431 needles. *J. Environ. Sci. Heal. B* 31(4), 671-698.
- 432 Baesman, S.M. and Miller, L.G. (2005) Laboratory determination of the carbon kinetic isotope
433 effects (KIEs) for reactions of methyl halides with various nucleophiles in solution. *J. Atmos.*
434 *Chem.* 52(2), 203-219.
- 435 Bashir, S., Hitzfeld, K.L., Gehre, M., Richnow, H.H. and Fischer, A. (2015) Evaluating
436 degradation of hexachlorocyclohexane (HCH) isomers within a contaminated aquifer using
437 compound-specific stable carbon isotope analysis (CSIA). *Water Res.* 71, 187-196.
- 438 Bondgaard, M., Hvidberg, B. and Ramsay, L. (2012) Remediation of pesticide contamination by
439 in situ alkaline hydrolysis - a new soil remediation technology, Monterey, California.
- 440 Coplen, T.B. (2011) Guidelines and recommended terms for expression of stable-isotope-ratio
441 and gas-ratio measurement results. *Rapid Commun. Mass. Sp.* 25(17), 2538-2560.
- 442 Coplen, T.B., Brand, W.A., Gehre, M., Groning, M., Meijer, H.A.J., Toman, B. and Verkouteren,
443 R.M. (2006) After two decades a second anchor for the VPDB delta C-13 scale. *Rapid*
444 *Commun. Mass. Sp.* 20(21), 3165-3166.
- 445 Elsner, M. (2010) Stable isotope fractionation to investigate natural transformation mechanisms
446 of organic contaminants: principles, prospects and limitations. *J. Environ. Monit.* 12(11),
447 2005-2031.

448 Elsner, M. and Imfeld, G. (2016) Compound-specific isotope analysis (CSIA) of micropollutants
449 in the environment - current developments and future challenges. *Curr. Opin. Biotechnol.* 41,
450 60-72.

451 FAO (1990) Parathion (58), Food and Agriculture Organization of the United Nations.

452 Fenner, K., Canonica, S., Wackett, L.P. and Elsner, M. (2013) Evaluating pesticide degradation
453 in the environment: blind spots and emerging opportunities. *Science* 341(6147), 752-758.

454 Hofstetter, T.B., Schwarzenbach, R.P. and Bernasconi, S.M. (2008) Assessing transformation
455 processes of organic compounds using stable isotope fractionation. *Environ. Sci. Technol.*
456 42(21), 7737-7743.

457 Hvidberg, B., Ramsay, L., Kirkegaard, C., Elkjær, L., Jorgensen, C., Oberender, A. and Kiilerich,
458 O. (2008) Remediation technologies for a large pesticide-contaminated site: enclosure,
459 alkaline hydrolysis and bioventing.

460 Junghare, M., Subudhi, S. and B., L. (2012) Improvement of hydrogen production under
461 decreased partial pressure by newly isolated alkaline tolerated anaerobe, *Clostridium*
462 *butyricum* TM9A: optimization of process parameters. *Int. J. Hydrogen. Energ.* 4(37), 3160-
463 3168.

464 Kawahara, J., Horikoshi, R., Yamaguchi, T., Kumagai, K. and Yanagisawa, Y. (2005) Air
465 pollution and young children's inhalation exposure to organophosphorus pesticide in an
466 agricultural community in Japan. *Environ. Int.* 31(8), 1123-1132.

467 Kopinke, F.D., Georgi, A., Voskamp, M. and Richnow, H.H. (2005) Carbon isotope
468 fractionation of organic contaminants due to retardation on humic substances: Implications
469 for natural attenuation studies in aquifers. *Environ. Sci. Technol.* 39(16), 6052-6062.

470 Liu, Y., Bashir, S., Stollberg, R., Trabitzsch, R., Weiss, H., Paschke, H., Nijenhuis, I. and
471 Richnow, H.H. (2017) Compound specific and enantioselective stable isotope analysis as
472 tools to monitor transformation of hexachlorocyclohexane (HCH) in a complex aquifer
473 System. *Environ. Sci. Technol.* 51(16), 8909-8916.

474 LRSB, L. (2014) Pilot experiments on the remediation technology in situ alkaline hydrolysis at
475 Groyne 42, Final report, NorthPestClean, Kongens Lyngby, Denmark.

476 Meckenstock, R.U., Morasch, B., Griebler, C. and Richnow, H.H. (2004) Stable isotope
477 fractionation analysis as a tool to monitor biodegradation in contaminated aquifers. *J.*
478 *Contam. Hydrol.* 75(3-4), 215-255.

479 Milosevic, N., Qiu, S., Elsner, M., Einsiedl, F., Maier, M.P., Bensch, H.K., Albrechtsen, H.J. and
480 Bjerg, P.L. (2013) Combined isotope and enantiomer analysis to assess the fate of phenoxy
481 acids in a heterogeneous geologic setting at an old landfill. *Water Res.* 47(2), 637-649.

482 Muff, J., MacKinnon, L., Durant, N.D., Bennedsen, L.F., Rugge, K., Bondgaard, M. and Pennell,
483 K. (2016) The influence of cosolvent and heat on the solubility and reactivity of
484 organophosphorous pesticide DNAPL alkaline hydrolysis. *Environ. Sci. Pollut. Res. Int.*
485 23(22), 22658-22666.

486 Nielsen, M.B., Kjeldsen, K.U., Lever, M.A. and Ingvorsen, K. (2014) Survival of prokaryotes in
487 a polluted waste dump during remediation by alkaline hydrolysis. *Ecotoxicology* 23, 404-
488 418.

489 Nijenhuis, I. and Richnow, H.H. (2016) Stable isotope fractionation concepts for characterizing
490 biotransformation of organohalides. *Curr. Opin. Biotechnol.* 41, 108-113.

491 NorthPestClean Projects related to the toxic waste site at Groyne 42
492 <http://www.eng.northpestclean.dk/publications/>.

493 NorthPestClean (2014a) Layman reports 2: Demonstration of in situ alkaline hydrolysis as a
494 novel soil remediation technique for a pesticide contamination, Central Denmark Region,
495 Department of Environment, <http://www.eng.northpestclean.dk/publications/layman-reports/>.

496 NorthPestClean (2014b) pilot experiments on the remediation technology in situ alkaline
497 hydrolysis at Groyne 42 - Final report,
498 [http://www.northpestclean.dk/publikationer/rapporter-fra-northpestclean-perioden-2011-
499 2014/](http://www.northpestclean.dk/publikationer/rapporter-fra-northpestclean-perioden-2011-2014/).

500 Pehkonen, S.O. and Zhang, Q. (2002) The degradation of organophosphorus pesticides in natural
501 waters: A critical review. *Crit. Rev. Env. Sci. Tec.* 32(1), 17-72.

502 Polatoğlu, İ., Yürekli, Y. and Baştürk, S.B. (2015) Estimating solubility of parathion in organic
503 solvents. *AKU J. Sci. Eng.* 15(3), 1-5.

504 Rokade, K.B. and Mali, G.V. (2013) Biodegradation of chlorpyrifos by *Pseudomonas*
505 *desmolyticum* NCIM 2112. *Int. J Pharm. Bio. Sci.* 2(4), (B) 609 - 616.

506 Schimmelmann, A., Qi, H.P., Coplen, T.B., Brand, W.A., Fong, J., Meier-Augenstein, W., Kemp,
507 H.F., Toman, B., Ackermann, A., Assonov, S., Aerts-Bijma, A.T., Brejcha, R., Chikaraishi,
508 Y., Darwish, T., Elsner, M., Gehre, M., Geilmann, H., Groing, M., Helie, J.F., Herrero-
509 Martin, S., Meijer, H.A.J., Sauer, P.E., Sessions, A.L. and Werner, R.A. (2016) Organic

510 reference materials for hydrogen, carbon, and nitrogen stable isotope-ratio measurements:
511 caffeines, n-alkanes, fatty acid methyl esters, glycines, L-valines, polyethylenes, and oils.
512 Anal. Chem. 88(8), 4294-4302.

513 Singh, B.K. and Walker, A. (2006) Microbial degradation of organophosphorus compounds.
514 Fems Microbiol. Rev. 30(3), 428-471.

515 Thatcher, G.R.J. and Kluger, R. (1989) Mechanism and catalysis of nucleophilic substitution in
516 phosphate esters. Adv. Phys. Org. Chem. 25, 99-265.

517 Thullner, M., Centler, F., Richnow, H.-H. and Fischer, A. (2012) Quantification of organic
518 pollutant degradation in contaminated aquifers using compound specific stable isotope
519 analysis – Review of recent developments. Org. Geochem. 42(12), 1440-1460.

520 USEPA (2006) Organophosphorus Cumulative Risk Assessment (2006 Update), pp. 1-189, U.S.
521 Environmental Protection Agency.

522 USEPA (2008) A guide for assessing biodegradation and source identification of organic ground
523 water contaminants using compound specific isotope analysis (CSIA). U.S. EPA Office of
524 Research and Development , N.R.M.R.L. (ed), p. 67, ADA OK.

525 Van Breukelen, B.M. (2007) Extending the Rayleigh equation to allow competing isotope
526 fractionating pathways to improve quantification of biodegradation. Environ. Sci. Technol.
527 41(11), 4004-4010.

528 Vogt, C., Dorer, C., Musat, F. and Richnow, H.H. (2016) Multi-element isotope fractionation
529 concepts to characterize the biodegradation of hydrocarbons - from enzymes to the
530 environment. Curr. Opin. Biotechnol. 41, 90-98.

531 Wanamaker, E.C., Chingas, G.C. and McDougal, O.M. (2013) Parathion hydrolysis revisited: in
532 situ aqueous kinetics by (1)h NMR. Environ. Sci. Technol. 47(16), 9267-9273.

533 Weber, K. (1976) Degradation of parathion in seawater. Water Res. 10(3), 237-241.

534 Wu, L., Chladkova, B., Lechtenfeld, O.J., Lian, S., Schindelka, J., Herrmann, H. and Richnow,
535 H.H. (2018) Characterizing chemical transformation of organophosphorus compounds by
536 (13)C and (2)H stable isotope analysis. Sci. Total. Environ. 615, 20-28.

537 Wu, L., Kummel, S. and Richnow, H.H. (2017) Validation of GC-IRMS techniques for delta C-
538 13 and delta H-2 CSIA of organophosphorus compounds and their potential for studying the
539 mode of hydrolysis in the environment. Anal. Bioanal. Chem. 409(10), 2581-2590.

540 Wu, L., Yao, J., Trebse, P., Zhang, N. and Richnow, H.H. (2014) Compound specific isotope
541 analysis of organophosphorus pesticides. Chemosphere 111, 458-463.

542

Table 1

[Click here to download Table: Table 1.docx](#)

Table 1. Physicochemical parameters of groundwater samples, parathion concentrations, parathion isotope values and qualitative assessment of *in situ* hydrolysis of parathion. Samples containing parathion concentrations below detection limit are not listed.

Well ID	water level (m)	Temp. (°C)	O ₂ (mg L ⁻¹)	conductivity (mS cm ⁻¹)	pH	sample volume (L)	Parathion (mg L ⁻¹)	δ ¹³ C (‰)	δ ² H (‰)	<i>In situ</i> hydrolysis at pH 2, 5 and 7 ^a (%)	<i>In situ</i> hydrolysis at pH 9 ^b (%)	C ₀ (mg L ⁻¹)
samples from treated area												
TC3-1-1	5.15	12.5	0.01	19.31	9.2	1.00	107.90	-23.6 ± 0.5	b.d.			
TC3-1-2	2.94	12.4	0.04	23.50	11.2	0.98	0.78	b.d. ^c	b.d.			
TC3-1-3	3.96	12.6	0.05	10.03	6.9	1.01	133.65	-22.8 ± 0.1	b.d.			
TC3-2-2	3.06	12.2	0.09	33.00	11.9	0.98	0.76	b.d.	b.d.			
TC3-2-3	3.04	12.4	0.04	12.70	10.3	0.98	1.37	b.d.	b.d.			
TC3-3-3	3.12	13.0	0.03	12.23	9.5	1.00	56.99	-22.1 ± 0.1	-210 ± 2			
TC3-6-3	3.19	12.6	0.04	12.51	11.7	0.98	5.75	-20.1 ± 0.4	b.d.	3.7 - 5.0	7.4 - 9.3	5.97 - 6.34
TC3-7-2	2.95	11.6	0.05	27.50	12.4	0.87	155.33	-20.8 ± 0.0	-227 ± 3	2.8 - 3.7	5.5 - 7.0	
TC3-7-3	2.97	12.2	0.05	12.26	8.1	0.94	124.46	-22.4 ± 0.2	-211 ± 6			
TC3-8-3	4.00	12.3	0.06	9.28	9.4	0.96	132.51	-23.0 ± 0.1	-201 ± 2			
TC3-9-3	3.07	12.2	0.11	13.91	2.2	1.00	33.97	-22.7 ± 0.1	-211 ± 2			
samples from untreated area												
T1-3-1	3.59	11.4	0.09	20.20	4.4	2.19	2.64	-22.1 ± 0.1	b.d.	1.1 - 1.4	2.2 - 2.7	2.67 - 2.72
TP2-1-1	1.40	11.4	0.07	5.47	3.8	2.18	3.22	-21.1 ± 0.3	b.d.	2.4 - 3.2	4.7 - 5.9	3.30 - 3.42
F5	3.81	12.7	0.08	5.46	4.1	2.00	3.16	-21.7 ± 0.2	-211 ± 1	1.6 - 2.1	3.1 - 3.9	3.21 - 3.29
V03-2	3.85	11.8	0.05	6.73	9.4	2.13	1.86	-21.7 ± 0.0	-215 ± 4	1.6 - 2.1	3.1 - 3.9	1.88 - 1.93
DGE15	3.88	12.0	0.08	6.81	4.0	2.33	4.94	-21.5 ± 0.6	-226 ± 0	1.8 - 2.4	3.6 - 4.5	5.03 - 5.17
V05 A	4.03	11.4	0.09	17.23	3.2	2.50	0.58	-18.3 ± 0.4	-208 ± 1	6.1 - 8.1	12.0 - 15.1	0.62 - 0.68
DGE13	3.51	12.5	0.10	9.34	6.5	2.50	0.01	-21.8 ± 0.0	b.d.	1.5 - 2.0	2.9 - 3.7	0.01 - 0.01
V81 B	3.49	12.4	0.10	14.64	3.5	2.27	0.12	-18.0 ± 0.6	-214 ± 5	6.5 - 8.6	12.7 - 16.0	0.13 - 0.14
^a quantitative assessment of <i>in situ</i> hydrolysis of parathion under neutral and acidic conditions using ε _C of -6.0 ± 0.2 at pH 7, ε _C of -6.7 ± 0.4 at pH 5 and ε _C of -6.9 ± 0.8 at pH 2. The ε _C values were obtained from lab experiments (Wu et al. 2018); ^b quantitative assessment of <i>in situ</i> hydrolysis of parathion under slightly alkaline condition using ε _C of -3.5 ± 0.4 at pH 9 obtained from (Wu et al. 2018) ; ^c b.d. : below detection limit.												

Figure 1_sampling map

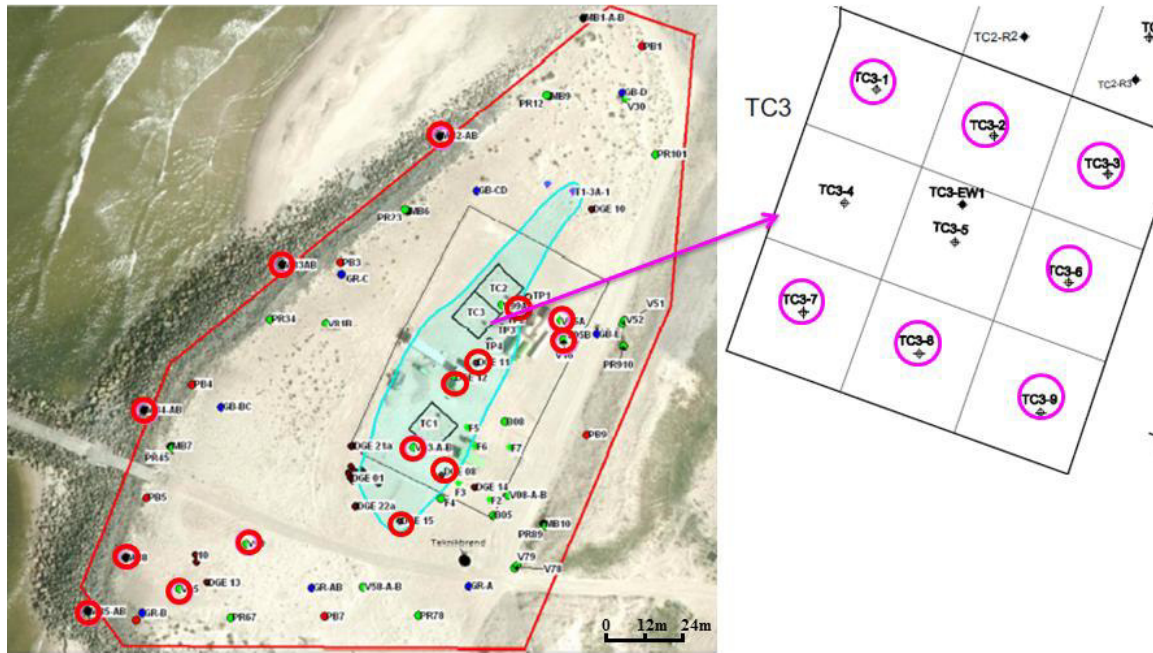


Fig. 1: Map of the “Groyne 42” field site showing the areas of *in situ* treatment by alkaline hydrolysis (TC1-TC3) and the locations of the sampling wells within the treated (pink circles) and untreated area (red circles). The area colored in blue indicates the location of the contamination hotspot.

Figure 2_Isotope ratio of field samples

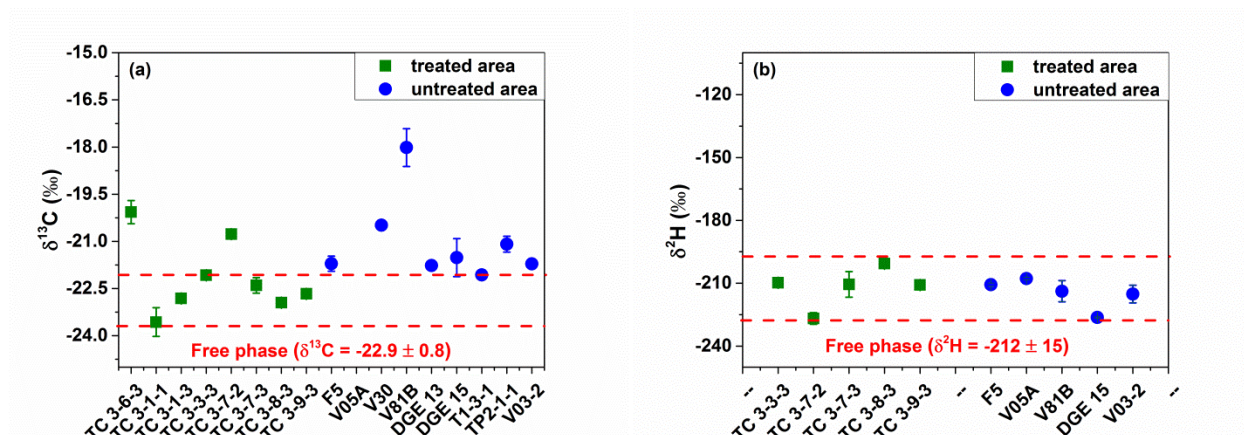


Fig. 2: Carbon (a) and hydrogen (b) isotope ratios of parathion obtained from the ground water from the “Groyne 42” field site. Green squares indicate the samples from the treated area; blue circles indicate the samples from untreated area; Red dotted lines indicate the carbon and hydrogen source signatures of parathion.

Figure 3_reaction scheme

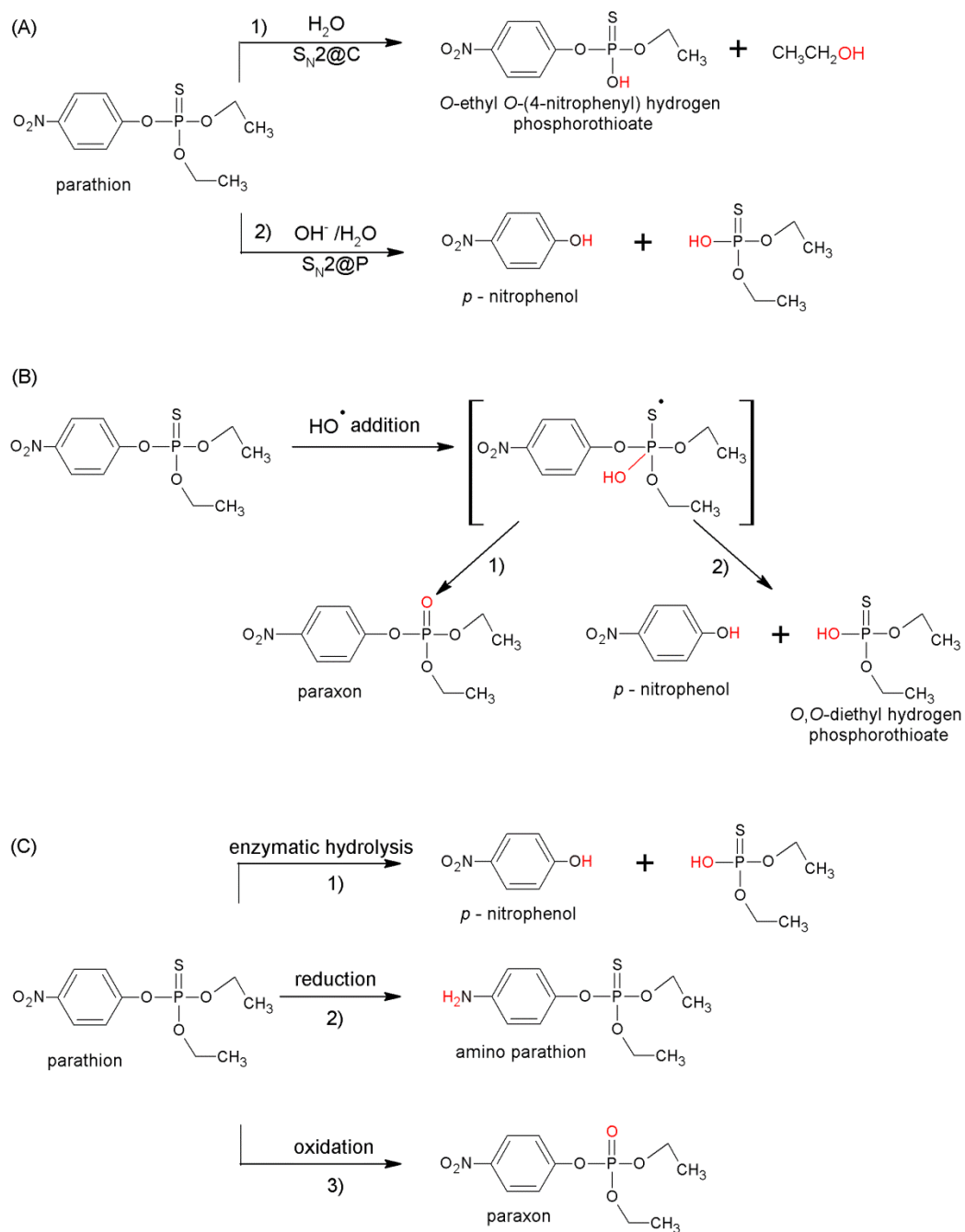


Fig. 3: Proposed reaction schemes with transformation mechanisms of parathion during (A) hydrolysis at different pH, (B) chemical oxidation by OH radical and (C) biodegradation.

Scheme (A) illustrates that hydrolysis of parathion occurs via two pathways: (A1) nucleophilic attack by H_2O at the α -carbon of the alkoxy group at acidic/neutral condition; (A2) nucleophilic

attack by OH^- and H_2O at the phosphorus atom at alkaline condition. Scheme (B) illustrates that the first rate-limiting step of the chemical oxidation of parathion by OH radical occurs via OH radical addition to the central phosphorus atom and stabilized by two different pathways: (B1) the elimination of sulfhydryl radical to produce P=O bond to form paraoxon; (B2) the elimination of nitrophenol from the phosphoric center to p-nitrophenol. Scheme (C) summarizes biodegradation pathways of parathion: (C1) enzymatic hydrolysis of the phosphotriester bond to form p-nitrophenol; (C2) reduction of the nitrogroup to form amino parathion; (C3) oxidation of parathion to paraoxon.

Figure 4_Arrhenius plot

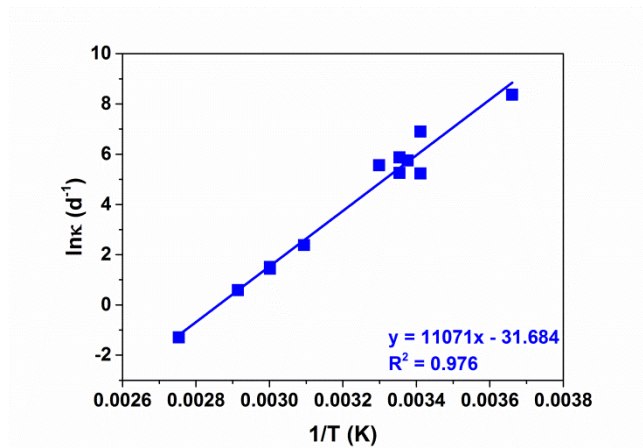


Fig. 4: The Arrhenius plot of parathion hydrolysis using collected data in Table S4.

Electronic Supplementary Material (for online publication only)

[Click here to download Electronic Supplementary Material \(for online publication only\): Supporting information_OP field study.c](#)